Engineering Geology 123 (2011) 40–59

Contents lists available at ScienceDirect

Engineering Geology

journal homepage: www.elsevier.com/locate/enggeo

# The formation and breach of a short-lived landslide dam at Hsiaolin village, Taiwan — part I: Post-event reconstruction of dam geometry

Jia-Jyun Dong [a,b,*], Yun-Shan Li [a], Chyh-Yu Kuo [c], Rui-Tang Sung [d], Ming-Hsu Li [d], Chyi-Tyi Lee [a], Chien-Chih Chen [b], Wang-Ru Lee [e]

[a] Graduate Institute of Applied Geology, National Central University, Jhongli, Taiwan
[b] Department of Earth Sciences, National Central University Jhongli, Taiwan
[c] Research Center for Applied Sciences, Academia Sinica, Taipei, Taiwan
[d] Graduate Institute of Hydrological and Oceanic Sciences, National Central University Jhongli, Taiwan
[e] Geotechnical engineering Research Center, Sinotech Engineering Consultants, Inc., Taipei, Taiwan

ARTICLE INFO

*Article history:*
Received 13 July 2010
Received in revised form 29 March 2011
Accepted 2 April 2011
Available online 12 April 2011

*Keywords:*
Landslide dam
Heavy-rainfall-triggered
Short-lived
Geomorphic characteristic
Overtopping
Failure mechanism

ABSTRACT

In this paper, technologies from multiple disciplines are used to reconstruct the shape of the Hsiaolin landslide dam, a short-lived landslide dam (SLD), that was triggered by Typhoon Morakot. Here, the formation, failure mode and breaching process of this SLD are investigated. The results indicate that the overtopping time and the debris budget constrained the dam geometry. The inferred volume of the Hsiaolin landslide dam (15.4 million $m^3$) is much smaller than the actual landslide volume (25.2 million $m^3$) even considering the rock-mass dilation and debris entrainment. Meanwhile, a 46% error could be induced if an over-simplified equation (a function of the dam height, length and width) is used to calculate the dam volume. The saddle of the dam crest, which is where overtopping occurred, could be used as a reference to measure the dam height and length. Accordingly, the determined dam dimensions of height (44 m), length (370 m) and width (1500 m) are suggested to be the representative geometrical indices that influenced the stability of the Hsiaolin landslide dam. The flow rate of the dammed river, another variable relevant to dam stability, was determined from a run-off simulation. It is suggested that, instead of the peak flow before the dam formation, the flow rate during the blockage period (2974 $m^3/s$) should be used as the training data for building a statistical model for stability predictions. Finally, the low hydraulic gradient at the toe of the dam's surface and the high safety factor of the dam slope indicate that the piping and slope instability were irrelevant to the failure of the Hsiaolin short-lived landslide dam. It is postulated that overtopping (about one hour after the blockage) dominated the failure process of this heavy-rainfall-induced landslide dam.



## 1. Introduction

### 1.1. Documenting the morphological characteristics of the landslide dam

Landslides may obstruct river flow and result in landslide dams. Such phenomena have occurred in many tectonically active regions of the world (e.g., Swanson et al., 1986; Costa and Schuster, 1988; Casagli and Ermini, 1999; Ermini and Casagli, 2003; Korup, 2004). The generation and disappearance of landslide-dammed lakes are the results of the interactions between a hill-slope and a valley-floor system. Understanding the processes involved in the formation and failure of landslide dams is crucial for the purpose of hazard mitigation, as well as for the reconstruction of ancient events and landscape evolution (Korup, 2002). However, landslide dams usually break down shortly after the formation of a landslide-dammed lake. Based on 63 cases from the literature, Schuster and Costa (1986) noted that "Many landslide dams maintain their integrity for only short periods of time — a few minutes to several days." Consequently, it is difficult to describe quantitatively the formation and breaching processes of a short-lived landslide dam (SLD), for which longevity ranged from a few minutes to several days.

There are two aspects that highlight the importance of completely and precisely documenting the morphological characteristics of an SLD and the related lake. Firstly, the current geomorphic approach is widely used to correlate the dam, river and water-storage characteristics with the stability of a landslide dam (Swanson et al., 1986; Costa and Schuster, 1988; Casagli and Ermini, 1999; Ermini and Casagli, 2003; Korup, 2004; Dong et al., 2009, 2011). However, the geomorphic data are incomplete and underreport small and ephemeral landslide dams while over-representing earthquake-related case studies (Korup, 2004). Therefore, adequate reporting of the formation and failing of a heavy-rainfall-triggered landslide dam is beneficial for understanding the

* Corresponding author at: Graduate Institute of Applied Geology, National Central University, Jhongli, Taiwan. Tel.: +883 3 4224114.
*E-mail address:* jjdong@geo.ncu.edu.tw (J.-J. Dong).

0013-7952/$ – see front matter © 2011 Elsevier B.V. All rights reserved.
doi:10.1016/j.enggeo.2011.04.001

impact of extreme weather on landslide dams. Secondly, detailed documentation of the processes of dam failure remains scarce (Korup, 2002), and any well-documented case example contributes to the field. To understand the breaching process and to simulate the catastrophic disasters caused by the outburst floods that frequently occur soon after the formation of a landslide-dammed lake, reconstructing the pre-failure dam geometry is required. In sum, gathering and restoring the morphological characteristics of a heavy-rainfall-triggered SLD through post-breach investigation are important both from the scientific and from the hazard-mitigation viewpoints.

### *1.2. Typhoon Morakot, the Hsiaolin landslide and the breach of the landslide dam*

In 2009, Typhoon Morakot brought intense rainfall to southern Taiwan and caused 17 landslides that resulted in the formation of dams (Chen and Hsu, 2009). One such landslide dam was located at the Hsiaolin village, Southern Taiwan (E120°38′39.1″, N23°10′0.6″; Figure 1). Hourly rainfall records from three nearby rainfall stations (solid circles in Figure 1) are shown in Fig. 2. A total of 2138 mm of accumulated rainfall was recorded at the Jiashian #2 rainfall station. The peak hourly rainfall intensity was 95 mm/h, and the rainfall duration was 99 h.

This extremely heavy rainfall triggered a catastrophic landslide with a volume of more than $20\times10^6$ m$^3$ that mainly comprised shale and colluvium (Lee et al., 2009). The huge landslide buried over one hundred houses in Hsiaolin village and entered the Cishan River, where a landslide-dammed lake was formed. Seismic waves induced by the landslide were registered by the Taiwan Central Weather Bureau Seismic Network (TCWBSN), and the occurrence time can be precisely identified as 06:16 a.m. on 9 August (local time) (Tsou et al., 2011). A vivid account was given by the eyewitness: "…a sudden loud rumbling bang and two small bangs were heard, and at this precise moment, the nearby Cishan River became completely dry and not a single drop of water was seen in the riverbed. Following the banging noises, there were only rock boulders scattered about the riverbed…" About an hour, this SLD collapsed. Overflowing floodwater washed away part of the buried village. The Hsiaolin landslide, the breached

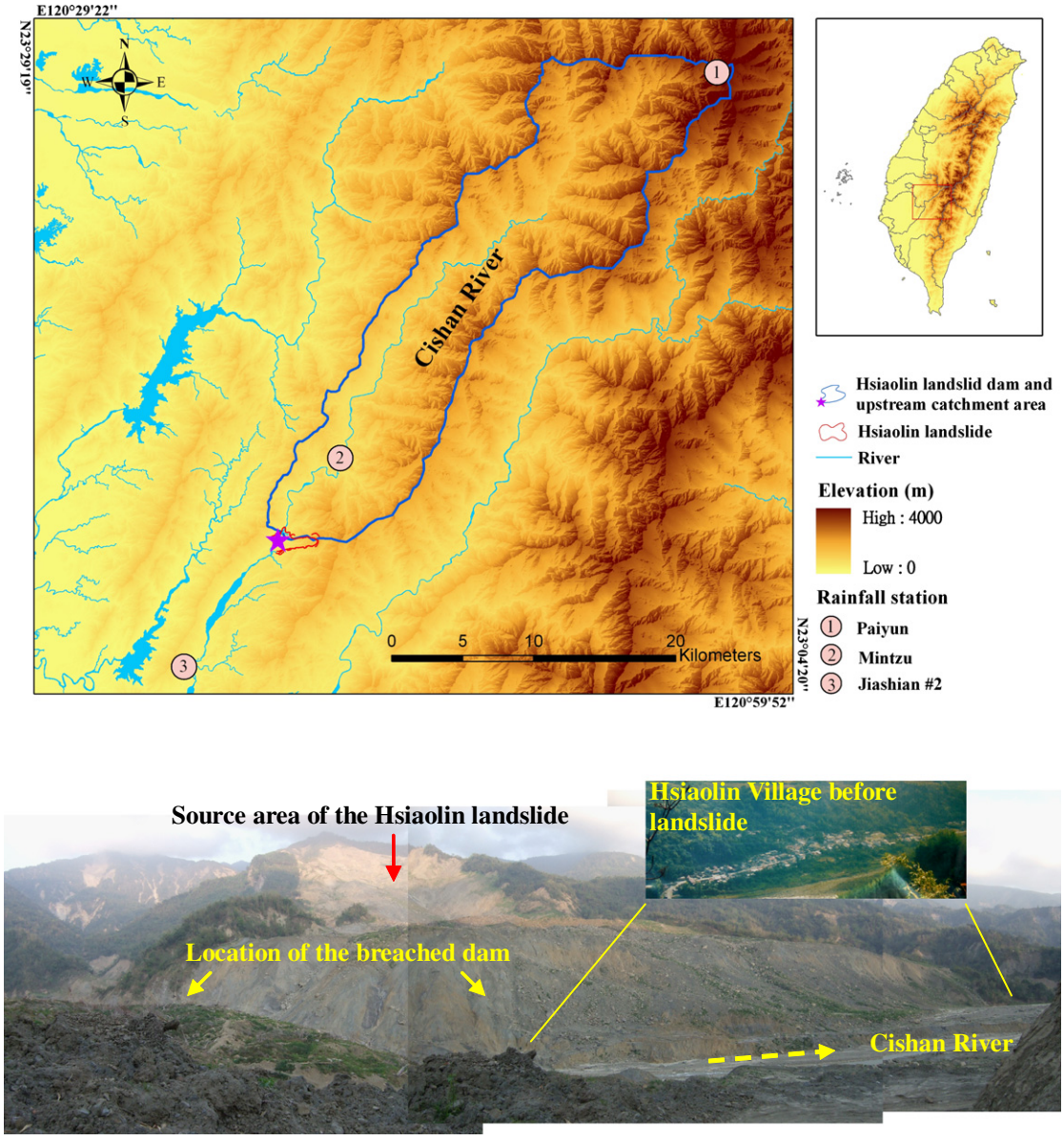


**Fig. 1.** The Hsiaolin landslide, the landslide dam and the buried Hsiaolin village. The landslide blocked the Cishan River and the landslide dam breached soon after the formation of an impounded lake. Blue line shows the drainage basin upstream of the Hsiaolin SLD. The boundary of the upstream catchment area is generated by the ArcHYDRO tool. The photo was taken from the west bank of the Cishan River shows the breached dam.

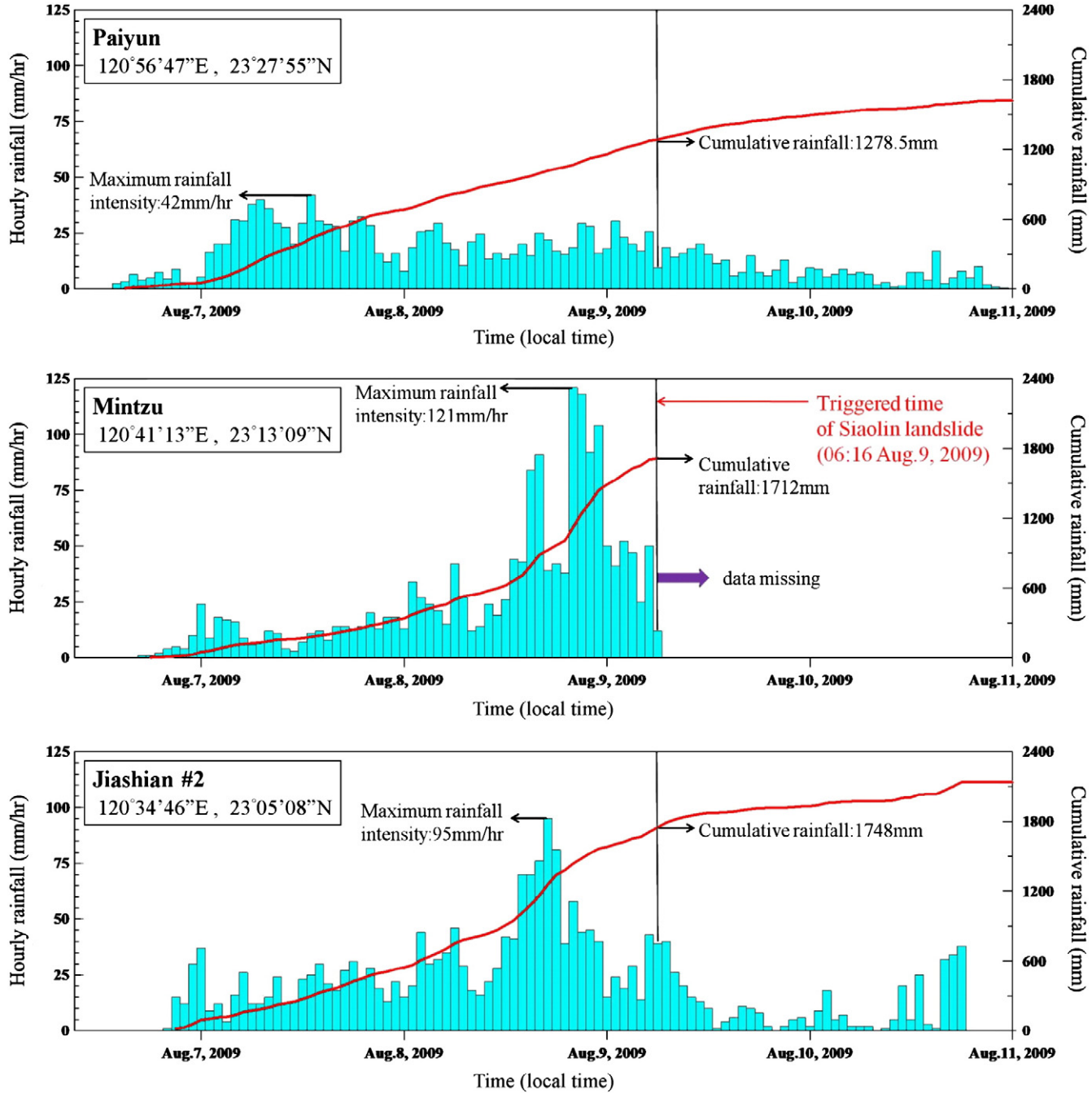


**Fig. 2.** The hourly rainfall record from rainfall stations (Paiyun, Mintzu and Jiashian #2) near the Hsiaolin landslide site during the 2009 Typhoon Morakot. Rainfall record of Paiyun station was collected from the Central Weather Bureau, Taiwan. Rainfall records of Mintzu and Jiashian #2 stations were collected from the Water Resources Agency, Taiwan.

landslide dam and the location of the buried Hsiaolin village are shown in Fig. 1.

### *1.3. Methodology for deriving the essential morphological characteristics of a landslide dam*

Schuster and Costa (1986) proposed that thirteen elements of information are essential for landslide–dam research (Table 1). These elements can be categorized into two types of data that pertain to: (1) landslide–dam formation and (2) the breaching process of a landslide dam. This paper (Part I) tries to elucidate how to gather and restore the information related to the formation of an SLD (items (a)–(j) in Table 1) from post-breach investigations. A companion paper (Part II) will reproduce the breaching process of the landslide dam (items (k)–(m) in Table 1).

Most of the information for items (a)–(j) can be easily obtained based on a geographic information system (GIS) if satellite images (or aerial photographs) and digital elevation models (DEMs) are available before and after the formation of a landslide dam. It is anticipated that, with the increasing availability of high-precision DEMs and high-resolution remote images, the capacity for reconstructing the formation and breaching processes of landslide dams will be greatly improved. However, the dimensions of a landslide dam (item (e)), which are generally relevant to the stability of landslide dams, are difficult to assess quantitatively if the dam is breached soon after its formation. Accordingly, the dimensions of impoundment (item (f))

**Table 1**
Essential information for landslide-dam research and commonly used technology for post-investigation.

| Elements of information on landslide dams[a] | Commonly used technology for post-investigation |
|---|---|
| 1. Formation of the landslide dam | |
| (a) Location and date of the landslide dam formation | Interpretation of satellite images and/or aerial photographs |
| (b) Type and characteristics of the landslide that formed the dam | Interpretation of satellite images and/or aerial photographs + digital elevation models + site investigations |
| (c) Surficial/bedrock geology in the source area of the landslide | Interpretation of satellite images and/or aerial photographs + site investigations |
| (d) Initial cause of the landslide if rainfall, intensity and duration data if earthquake, magnitude | Rain gages and/or seismograms |
| (e) Height, width, length and volume of the landslide dam[b] | Digital elevation models and/or eyewitnesses |
| (f) Length, width, depth and volume of the impoundment[b] | digital elevation models and/or eyewitnesses |
| (g) Physical characteristics of the geological materials that comprise the dam | Site investigations + geophysical explorations + in-situ and/or laboratory tests (if part of the breached dam still exists) |
| (h) Presence of seepage, piping, or slope failure on the faces of dam[b] | Site investigation and/or eyewitnesses |
| (i) Longevity of the landslide dam and impoundment[b] | Monitoring and/or eyewitnesses |
| (j) Mechanism(s) of failure of the landslide dam (if applicable)[b] | Site investigations + geophysical explorations + in-situ and/or laboratory tests (if part of the breached dam still exists) + seepage flow and slope stability analysis |
| 2. Breaching processes of the landslide dam | |
| (k) Characteristics of the breach | Monitoring and/or simulations |
| (l) Estimation or measurement of peak discharge | Monitoring and/or simulations |
| (m) Attenuation of the flood-wave downstream | Monitoring and/or simulations |

[a] Referring to Schuster and Costa (1986).
[b] Difficult to assess quantitatively for an SLD.

are also difficult to assess. Moreover, the longevity of the dam/lake (item (i)), the presence of seepage, piping, or slope failure on the faces of the dam (item (h)) and the dam's failure mechanism (item (j)) are difficult to evaluate for an SLD for which the DEM from before dam breaching is unavailable.

The objective of this study is to reconstruct the formation process and geometry of the breached Hsiaolin landslide dam using a multidisciplinary approach. For a landslide dam as short-lived as was the one at Hsiaolin, DEMs from before the landslide and after dam breaching are sometimes available. However, it is nearly impossible to obtain the "true" topography of an SLD before the dam breach. This fact limits the capacity to reconstruct quantitatively the geometry of the breached landslide dam. In this research, geomorphology, geology, engineering geology and hydrology approaches were adopted to reproduce the geometry of the Hsiaolin landslide dam. Aerial photographs taken before and after Typhoon Morakot, 5-m-resolution digital terrain models (DEMs) and extensive fieldwork were utilized in the investigation. Based on the aerial photographs and DEMs, the total volume of the landslide could be estimated. In addition, the debris entrainment was calculated using the DEMs before and after the landslide. A fractional amount of volume expansion of the sliding rock mass was introduced when estimating the volume of debris forming the landslide dam. Field-based evidence, as well as the estimated dam-crest height constrained by the overtopping time, was used to infer the dam geometry. Accordingly, seepage and slope stability analyses using the reconstructed dam geometry were conducted to evaluate the possible failure mechanism. Based on this case history, a standard description of the morphological characteristics related to a landslide dam is highlighted. The reliability of the reconstructed characteristics of the short-lived landslide dam is also elucidated. The breaching process of the landslide dam is documented in a companion paper (Part II) in this issue (Li et al., this issue). The flow chart of the presented Hsiaolin landslide-dam-related research (Part I and Part II) is summarized in Fig. 3.

## 2. Aerial photograph interpretation and site investigations

Part of the breached Hsiaolin landslide dam can still be clearly identified from a high-resolution aerial photograph taken by the Aerial Survey Office, Forestry Bureau, Taiwan after Typhoon Morakot (Figure 4). The aerial photograph, together with the high resolution DEMs, reveals valuable information about the pre-breach geometry of the Hsiaolin landslide dam.

First, the Hsiaolin landslide had two main tracks along creeks A and B that can be clearly identified from the aerial photograph. The debris that formed the breached dam traveled mainly along creek A. The debris volume contributed from creek B might not be directly related to the landslide dam.

Second, the stripped surfaces of the west bank of the Cishan River indicate the action of the landslide run-up, the debris deposition (dam site), the impounded water level of the landslide-dammed lake (upstream) and the breaching flow (downstream) on the slope. Therefore, the highest elevation of the uncovered area on the west bank indicates the upper boundary of the dam crest. Notably, it can be observed from Fig. 4 that the upper boundary of the stripped area on the west bank is at Ele. 475 m (short dash line). This bare area may be the result of super-elevation of high-speed debris.

Abundant driftwood on the downstream side of the breached dam indicates flood modification after the dam breach. However, driftwood is absent from a higher terrace (the boundary is marked with a long dash line in Figure 4). The higher terrace therefore could be the part of the landslide dam that was not overtopped by the flood.

Field observations from upstream of the breached dam showed only minor damage on the east bank (Figure 5). It is postulated that, because the road is not buried by the landslide, it can be adopted as a constraint for the reconstruction of the dam geometry. In addition to sticks found hanging on the light at the tunnel, lake deposits of poorly sorted sand with few fines were found on the roof of a nearby house (Figure 6). This is evidence that the impounded water level exceeded Ele. 410 m. Fig. 7 shows another house at Ele. 440 m in which evidence of water was found. Consequently, the impounded water level should possibly have been between Ele. 410–440 m.

Fig. 8(a)–(d) shows the west bank of the breached dam. The top of the deposit was covered with large sandstone blocks (Figure 8(a)). Sandstone blocks of several meters in diameter were abundant. The materials on the lower part of the dam were relatively dense indicating severe compaction (Figure 8(b)). The dam materials were mainly composed of fine particles of less than 2 mm diameter (Figure 8(c)). Abundant shale fragments with diameters of up to 1 m were observed in a fine-grained matrix-supported structure. Notably, Fig. 8(d) shows several gullies that were eroded by the surface run-off. This implies that the fine-grained dam materials were relatively erosive. Interestingly, the dam materials are very similar to the materials observed on the slope (Figure 9). It is speculated that either

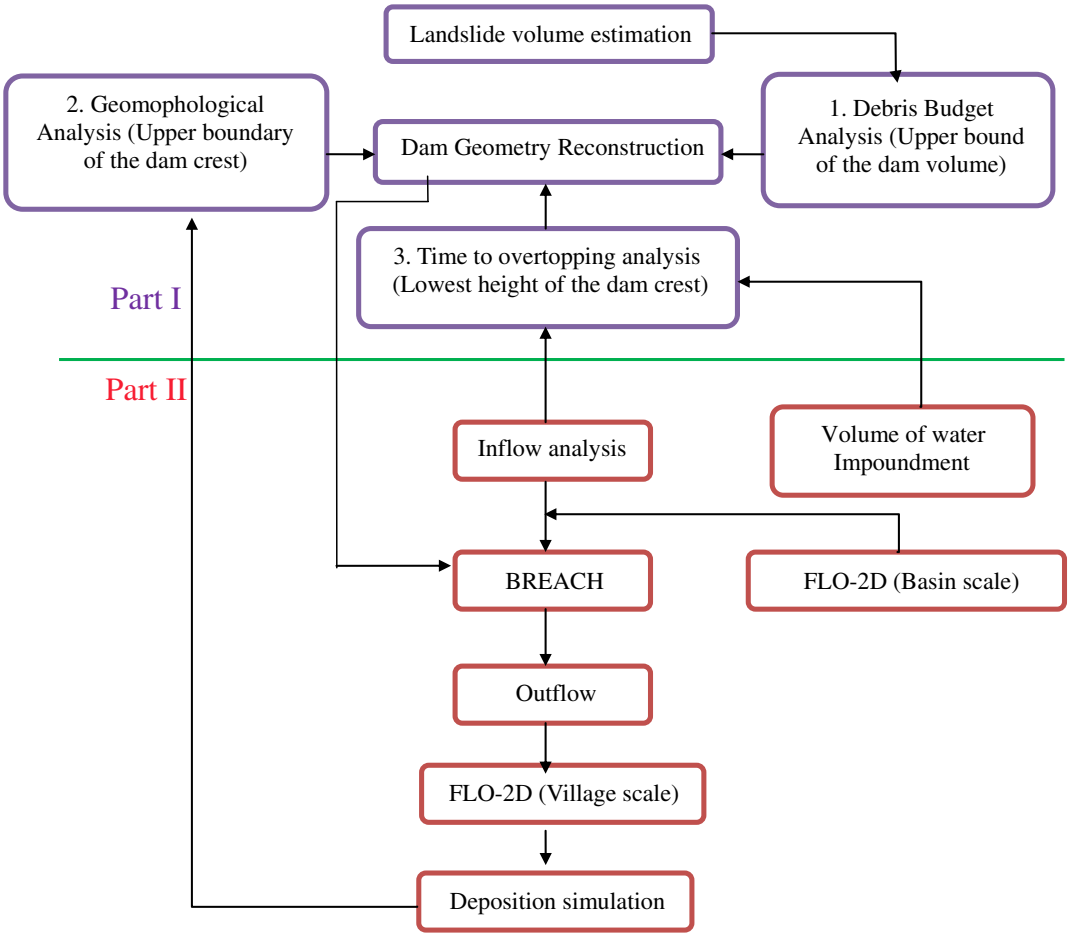


**Fig. 3.** Flow chart for the research related to the Hsiaolin SLD study.

the shale formation was highly sheared or that there was abundant fine-particle colluvium deposited at the source area before the catastrophic landslide event.

## 3. Laboratory work

Field observations indicate that the matrix of the dam materials was composed of sand, silt and clay particles. Consequently, the grain-size analysis was conducted in the laboratory instead of using analysis based on field measurements as suggested by Casagli et al. (2003). Four samples of landslide deposits were selected from the west bank (Figure 8) of the breached dam. Particles with sizes greater than a 4# U.S. sieve (4.75 mm) were extracted, and laboratory sieve and hydrometer analyses were used to determine the grain-size distributions of the dam materials (Figure 10). The wet unit weight ($\gamma_t$), water content ($W_w$), specific gravity ($G_s$), Atterberg Limits and fines content ($F_c$) of the dam materials are listed in Table 2. The averaged wet unit weight of the dam materials was 20.9 kN/m$^3$. Five colluvium samples that remained at the source area were also collected. The average wet unit weight of the colluvium at the source area was 19.0 kN/m$^3$. The slightly greater unit weight of the dam material than that of the colluvium that remained on the slope indicates a dynamic compaction effect caused by the deposition of an enormous and fast-moving mass.

The matrix of the dam material was classified as SC, SM and CL according to the Unified Soil Classification System (USCS). The high fines content (38–51%) in the matrix of the dam material implied that its behavior is dominated by fine particles (silt or clay). The effective size ($D_{10}$) ranged from 0.002 to 0.005 mm, which is very close to the size of clay particles. This low effective size of the dam material is far below the grain size for which Hazen's equation can be applied to estimate the hydraulic conductivity (Hazen, 1930). For silty–clayey sands, the hydraulic conductivity ranges from $10^{-3}$to $10^{-6}$ cm/s (Fetter, 1994).

The results of the laboratory work and field observations of the dam materials highlighted two points, as follows: (1) most of the dam body (lower part) was relatively impermeable, whereas the upper part of the dam (several meters) was composed of loosely packed blocks with clastic-supported structures that could have been highly permeable; (2) the erosion resistance might have been quite different for the upper and lower parts of the landslide dam.

Meanwhile, we also sampled some lake deposition upstream of the breached dam. The mean particle diameter ($D_{50}$) of the deposition materials was 0.2 mm. The coefficients of uniformity ($C_u = 2.7$) and curvature ($C_d = 5.1$) indicate that the particle distribution of the lake deposition was relatively uniform and poorly sorted.

## 4. Debris budget — constraints on the estimation of dam volume

### 4.1. Debris budget

If DEMs from before the formation and breaching of a landslide dam are available, then the dam volume and geometry can be calculated directly. For a rapidly breached dam, however, the dam volume is generally estimated indirectly from the volume of the landslide. Several factors might affect the estimation of the volume of a landslide dam ($V_d$) from the volume of a landslide. Firstly, the fragmentation of rocks and the entrainment of substrate material on the moving path of a landslide might increase the volume of

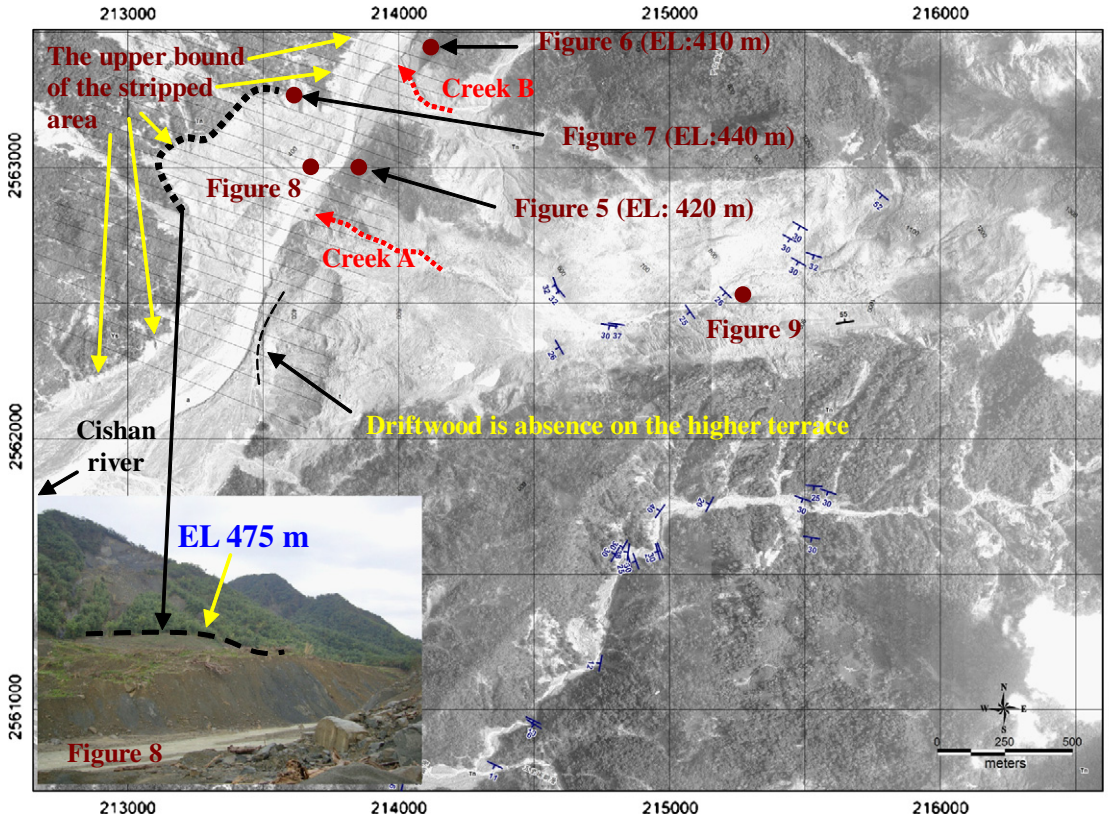


**Fig. 4.** Aerial photograph taken by the Aerial Survey Office, Forestry Bureau, Taiwan after Typhoon Morakot. The aerial photograph was taken at August 22, 2009, about two weeks after the Hsiaolin landslide. Around the dam area, vegetation only exists at elevations higher than 475 m above sea level. Elevation decreases to about Ele. 420 m both upstream and downstream of the dam and on the west bank of the Cishan River. This indicates that the super-elevation of the landslide deposits might have been caused by high-speed debris.

the landslide deposits compared to the initial volume of the landslide. Hungr and Evans (2004) suggested that the total volume of landslide deposits equals $V_{ls,i} \cdot (1+F_F)+V_E$, where the $V_{ls,i}$ is the initial volume of a landslide, $F_F$ is the fractional amount of volume expansion due to rock fragmentation and $V_E$ is the volume of the entrained materials.

Secondly, some sliding material that did not contribute to the volume of the landslide dam might be deposited on the slope ($V_{ls,slope}$).


**Fig. 5.** The slightly damaged road immediately upstream of the landslide dam on the east bank of the Cishan River.


**Fig. 6.** Lake deposit of poorly sorted sand could be found in the roof of a house located on a terrace at Ele. 410 m. In addition, there were sticks hanging at the top of the tunnel near the house. Therefore, the minimum-possible impounded water level of the dammed-up lake was approximately Ele. 410 m.

Accordingly, the volume of the landslide deposits that entered the river channel ($V_{ls,channel}$) could be estimated by:

$$V_{ls,channel} = V_{ls,i}\cdot(1 + F_F) + V_E - V_{ls,slope}. \quad (1)$$

Thirdly, the portion of the landslide deposits that entered the river channel might be delivered downstream, especially if the landslide was triggered by heavy rainfall. As the Hsiaolin landslide was triggered by heavy rainfall, a portion of the landslide materials might have been


**Fig. 7.** Water traces were found in a house at about Ele. 440 m. Therefore, the maximum-possible impounded water level of the natural lake was Ele. 440 m.

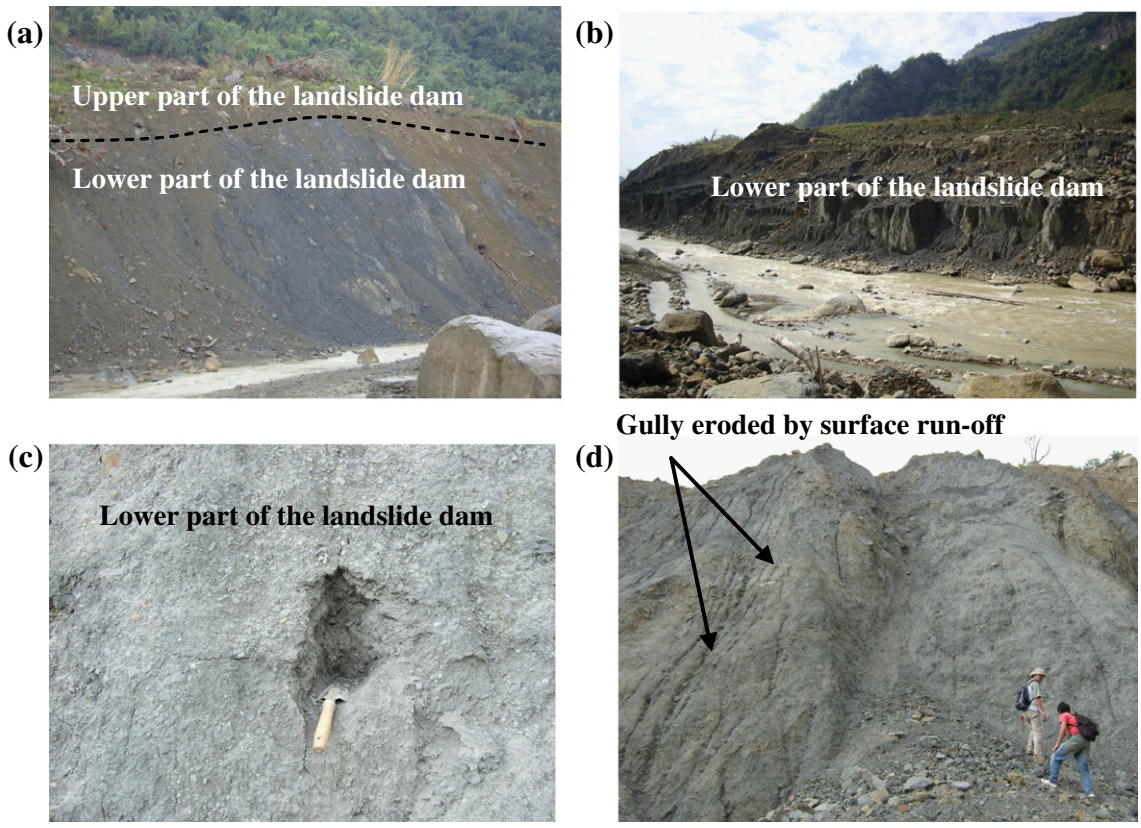


**Fig. 8.** Part of the relic dam on the west bank of the Cishan River. (a) An overview of the relic dam. The photograph was taken from upstream on the east bank to downstream on the west bank. (b) A closer-up view of the relic dam. The photograph was taken from the east bank to the west bank near the intersection of Creek A and the Cishan River. (c) A close-up view of photograph (b), in which the dam materials show a matrix-support structure with small shale blocks floating on the fine particles.

transported downstream by the high discharge in the Cishan River. In that case, the transported portion did not contribute to the volume of the landslide dam. In addition, the Hsiaolin landslide traveled down two main paths along creeks A and B (Figure 4). The debris from Creek B did not contribute to the volume of the main body of the Hsiaolin landslide dam. The fractional amount ($F_w$) that accounts for the contribution of

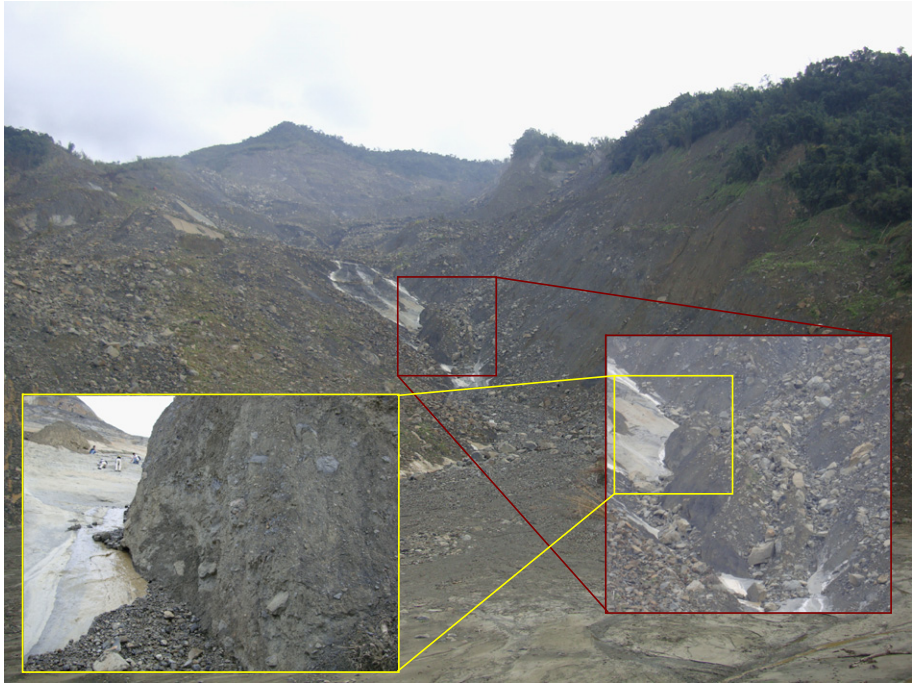

**Fig. 9.** Sliding materials remained on the slope. The materials were mainly composed of fine particles mixed with some shale blocks and are similar to the materials of the landslide dam.

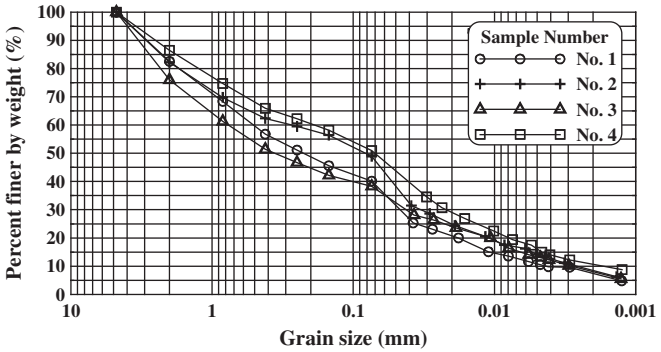


**Fig. 10.** Grain-size distribution curves of the dam material.

the landslide deposits that entered the river channel and contributed to the volume of landslide dam was introduced as follows:

$$V_d = (1-F_w)\cdot V_{ls,channel}. \quad (2)$$

However, the estimation of $F_w$ in Eq. (2) is difficult for a rapidly breached landslide dam. Generally, the value of $F_w$ ($0 \le F_w < 1$) is dominated by the flow rate of the discharge, namely the landslide velocity and the characteristics of the dam materials. An assumption of $F_w = 1$ is that all of the debris was washed away by the run-off flowing in the river. At the same time, $F_w = 0$ indicates that the dam volume equaled the volume of the landslide deposits that entered the river channel ($V_{ls,channel}$). That is, the volume of the landslide deposits that entered the blocked river channel can be treated as the upper bound of the dam volume. Finally, the volume of the landslide dam can be estimated by combining Eqs. (1) and (2).

### 4.2. Estimating the volume of debris that entered the channel ($V_{ls,channel}$)

Changes in the elevation before and after Typhoon Morakot (Figure 11) were derived from two 5-m-resolution digital terrain models (DEMs) with a vertical precision of about 2.5 m (provided by the Aerial Survey Office, Forestry Bureau, Taiwan). Based in Fig. 11, the net-volume changes cause by the landslide ($V_{ls,i}$), the entrainment of substrate material ($V_E$) (with decreased elevation) and the debris deposition on slope ($V_{ls,slope}$) (with increased elevation) can be calculated precisely. Accordingly, the volume of the major landslide body (area L in Figure 11 with a sliding depth that exceeds 5 m) is about $25.2\times10^6$ m$^3$. The entrainment of substrate material $V_E$ (areas E in Figure 11 with a substrate depth that exceeds 5 m) is about $2.2\times10^6$ m$^3$. Excluding the areas L and E, the volume of debris deposition on slope $V_{ls,slope}$ is about $15.4\times10^6$ m$^3$.

To reasonably calculate the volume of landslide deposits that entered the channel (Eq. (1)), the estimation of the fractional amount of volume expansion due to fragmentation ($F_F$) is critical. As stated previously, two kinds of materials were identified at the source area; these included the Pliocene shales overlain by colluvium. Two geological profiles of the landslide area are illustrated in Fig. 12, and the locations of the profiles are shown in Fig. 11. Based on the measured porosity of loosely placed, well-graded crushed rocks, Hungr and Evans (2004) proposed a 25% volume expansion caused by rock fragmentation. Based on high-resolution DEM data, Chang et al. (2006) reported that the average density of the debris deposit of the Jiufengershan landslide in Central Taiwan was about 17% less than the density of the original rocks. That is, the sliding mass of the Jiufengershan landslide (which was mainly composed of Early-to-Middle Miocene shales with alternations of sandy silts and shales) expanded 17% due to rock fragmentation. Chen et al. (2006) reported a decompaction coefficient of 19–22% for the sliding Pliocene-aged Cholan formation (mainly composed of sandstone and shale). Accordingly, a decompaction coefficient of 20% was used to estimate the volume expansion due to the fragmentation of the Pliocene Yanshuikeng shale that is outcropped in the source area of the Hsiaolin landslide.

**Table 2**
Laboratory-test results of the materials comprising the Hsiaolin SLD.

| Samples no. | 1 | 2 | 3 | 4 |
|---|---|---|---|---|
| Wet unit weight $\gamma_t$ (kN/m$^3$) | 20.1 | 20.6 | 21.3 | 21.7 |
| Nature water content $W_w$ (%) | 3.4 | 1.7 | 1.8 | 1.8 |
| Specific gravity $G_s$ | 2.85 | 2.56 | 2.80 | 2.71 |
| Atterberg limits (%) | LL = 24.1<br>PI = 7.5 | LL = 23.1<br>PI = 3.6 | LL = 25.6<br>PI = 7.7 | LL = 29.5<br>PI = 7.8 |
| Fines content $F_c$ (%) | 40 | 49 | 38 | 51 |
| Soil classification | SC | SM | SC | CL |
| Medium size, $D_{50}$ (mm) | 0.24 | 0.09 | 0.40 | 0.07 |
| Hazen's effective size, $D_{10}$ (mm) | 0.005 | 0.003 | 0.003 | 0.002 |

Estimation of the volume changes of the colluvium at the source and deposition areas is also important. According to the laboratory analysis, the wet unit weight of the colluvium on the slope is similar to that of the dam materials. Therefore, we assumed that the colluvium presented no volume expansion. If the fractions of colluvium and shale at the source area of the Hsiaolin landslide can be determined, the averaged fractional amount of volume expansion due to fragmentation ($F_F$) can be estimated without difficulty. Based on the site investigation results, it was suggested that abundant colluvium might have existed at the source area before the landslide (Lee et al., 2009). We assumed that the volume of shale equaled twice the volume of colluvium at the source area (Figure 12). Consequently, the averaged fractional amount of volume expansion due to fragmentation ($F_F$) is about 13%. From Eq. (1), the volume of landslide deposits that entered the channel $V_{ls,channel}$ was estimated to be $15.3\times10^6$ m$^3$.

### 4.3. Estimation of the dam volume

To estimate the dam volume $V_d$ (Eq. (2)), the fractional amount ($F_w$), which accounts for the contribution of landslide deposits that entered the channel of the landslide dam, should be estimated. However, because the dam has already breached, it is difficult to estimate $F_w$. At this stage, the estimated $V_{ls,channel} = 15.3\times10^6$ m$^3$ is assumed to be the maximum dam volume. The uncertainty for estimating dam volume that results from the unknown $F_w$ will be further discussed in Section 6.

## 5. Time to overtopping — constraints on the estimation of dam height

The elevation of the inferred dam crest should be closely related to the highest water level of the impounded lake. However, only vague information related to the highest water level of the impoundment is available. Field evidence indicated that the highest water level might have ranged between 410 m and 440 m in elevation. Eyewitnesses documented that the water reached as far as the No. 11 Bridge where the elevation is 425–430 m (Li et al., this issue; Figure 8). Furthermore, the eyewitnesses estimated that the overtopping of the landslide dam began at about 07:00 a.m., which was approximately 44 min after the landslide began at 06:16 a.m. Feng (2011) estimated the landslide dam breached at around 07:40 a.m. (84 min after its forming) based on the broadband seismograms data. Therefore, the overtopping time should be less than 84 min." In addition, please add one reference in the reference list: "Feng, Z. Y., Personal communications, 2011. The breaching time of the Hsiaolin landslide dam could also be constrained by the time of peak discharge recorded downstream. A peak discharge about 3 h after the formation of the landslide dam was recorded by a streamflow station (Shanlin Bridge) 30 km downstream of the landslide dam site. In the companion paper (Part II), the results of a 2D rainfall-runoff simulation over the Cishan River basin indicate that two hours (Figure 6 in Li et al., this issue) is required for the peak discharge travel from the landslide dam site to the Shanlin Bridge station. Therefore, the collapse of SLD could be estimated as about an hour after its formation. In addition, the numerical

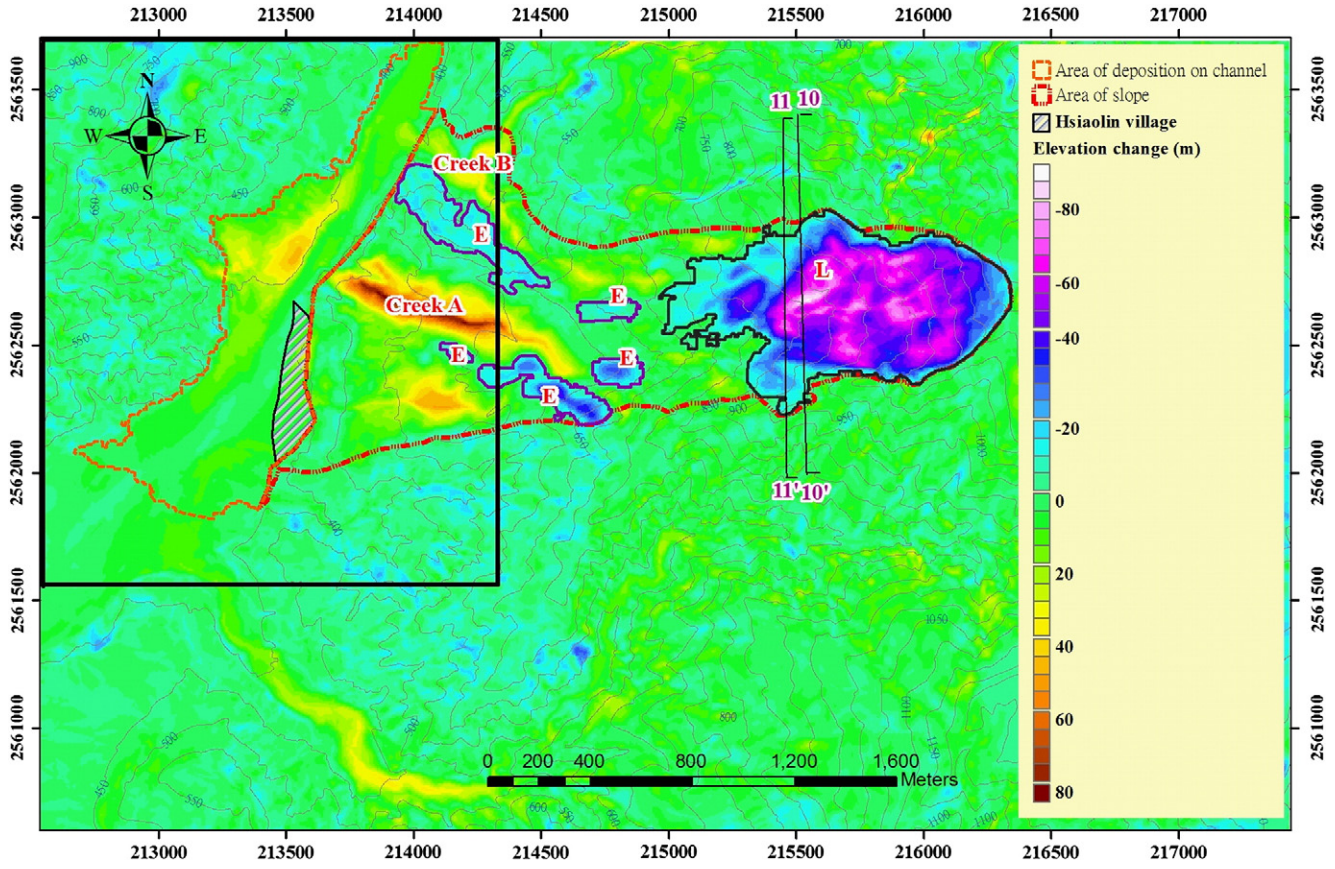


**Fig. 11.** Elevation changes in the ground surface after Typhoon Morakot. This figure is derived from two periods of high-resolution DEMs. The landslide area with a sliding depth of greater than 5 m and the area with a substrate depth of greater than 5 m are marked as L and E, respectively. The estimated volumes of the landslide and entrainment are about $25.2\times10^6$ m$^3$ and $2.22\times10^6$ m$^3$, respectively. The volume of the debris deposition on slope is about $15.4\times10^6$ m$^3$.

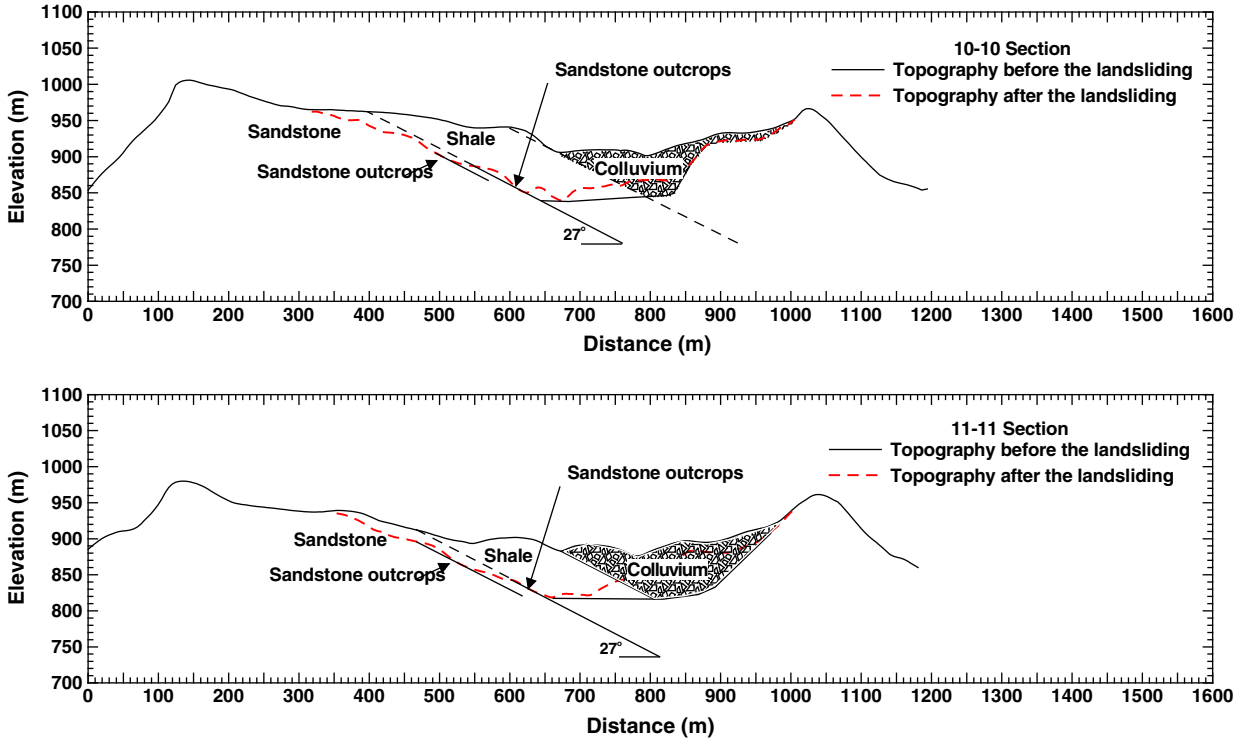


**Fig. 12.** Geological profiles of the Hsiaolin landslide. The locations of these two cross-sections are shown in Fig. 11.

simulation shows the upstream inflow rate during the presence of the SLD was 2974 $m^3/s$. Consequently, the time for overtopping and the estimated inflow rate could together provide an important constraint on the elevation of the dam crest, which is closely related to the highest water level of the landslide-dammed lake. Simulated hydrographs for rainfall-runoff during Typhoon Morakot can be found in this issue (Figure 6 in Li et al., this issue).

The water-storage volume of the landslide-dammed lake versus the elevation of the impounded water level can be calculated based on the DEM from after the Typhoon Morakot event. Under the simulated discharge (2974 $m^3/s$ at 06:00 a.m.), more than 3 h are required for overtopping if the dam crest where the overtopping occurred is at Ele. 440 m. An overtopping time of 44 min and 84 min after the formation of the dam indicates that the elevation of the dam crest where the overtopping occurred was 410–420 m. The uncertainty of the inferred dam geometry that is associated with the time to overtopping will be discussed later.

## 6. Reconstruction of the shape of the landslide dam

For establishing the shape of an SLD, three topographic datasets are essential. These are: (1) the pre-landslide topography; (2) the post-landslide topography; and (3) the post-dam-breach topography. The topography changes in channel between periods (1) and (2) represent the landslide-dam shape. The elevation difference between the topography of periods (2) and (3) indicates the breached part of the landslide dam.

The topography of periods (1) and (3) was derived from the DEMs. Fig. 13 shows a close-up view of the area marked in Fig. 11 (near the breached dam), which indicates the variation in the topography before the formation of the landslide dam and after its breach. Thirty-one cross-sections that are perpendicular to the river are indicated in the figure and represent the topography of period (2).

### 6.1. Reconstruction of topography after the landslide and before the dam breach

To reconstruct the dam geometry, field evidence (Section 2), constraints related to the time to overtopping (Section 5) and the debris budget (Section 4) were considered. Firstly, the elevation of the upper boundary of the bare rocks was carefully marked on the topographic map with the overlapping of the aerial photo that was taken after the dam breach as the upper boundary of the crest of the breached dam. Secondly, Ele. 415 m was selected as the dam crest where the overtopping occurred. Finally, we fine-tuned the geometry of the dam to balance the debris volume of the landslide and the landslide dam.

Fig. 14 shows the reconstructed dam geometry. The ground surfaces from before the formation of the landslide dam and from after the breach of the dam are indicated as solid black lines and dash red lines, respectively. Most of the topography remained unchanged before and after the landslide. Some of the topography of the west bank (right side of the profiles) varied slightly due to shallow landslides. Significant variation of the topography of the east bank

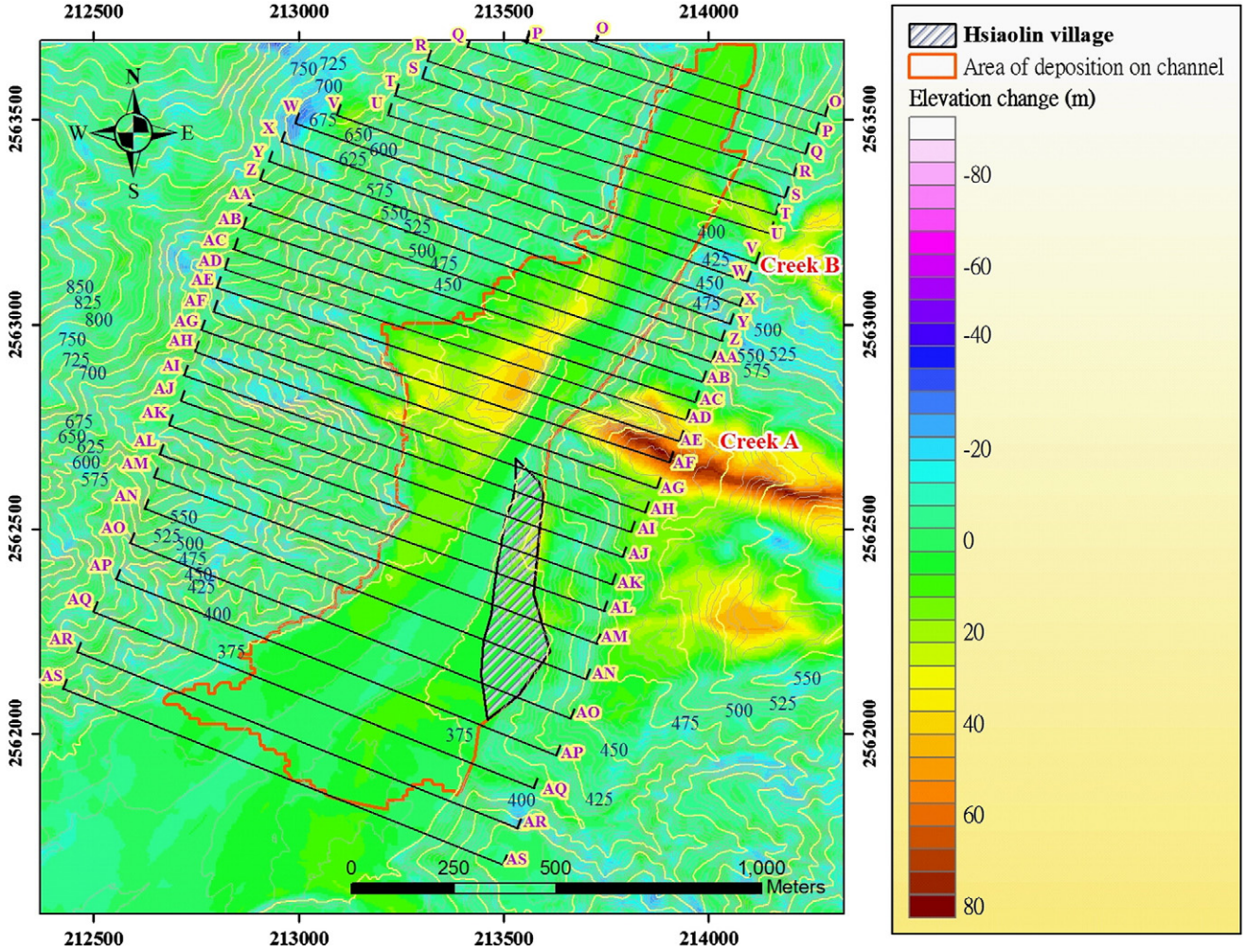


**Fig. 13.** A close view of the marked square area in Fig. 11 in the vicinity of the breached dam showing the topography changes before and after Typhoon Morakot. The locations of the 31 cross sections and one profile along the river (A-A′) are also marked.

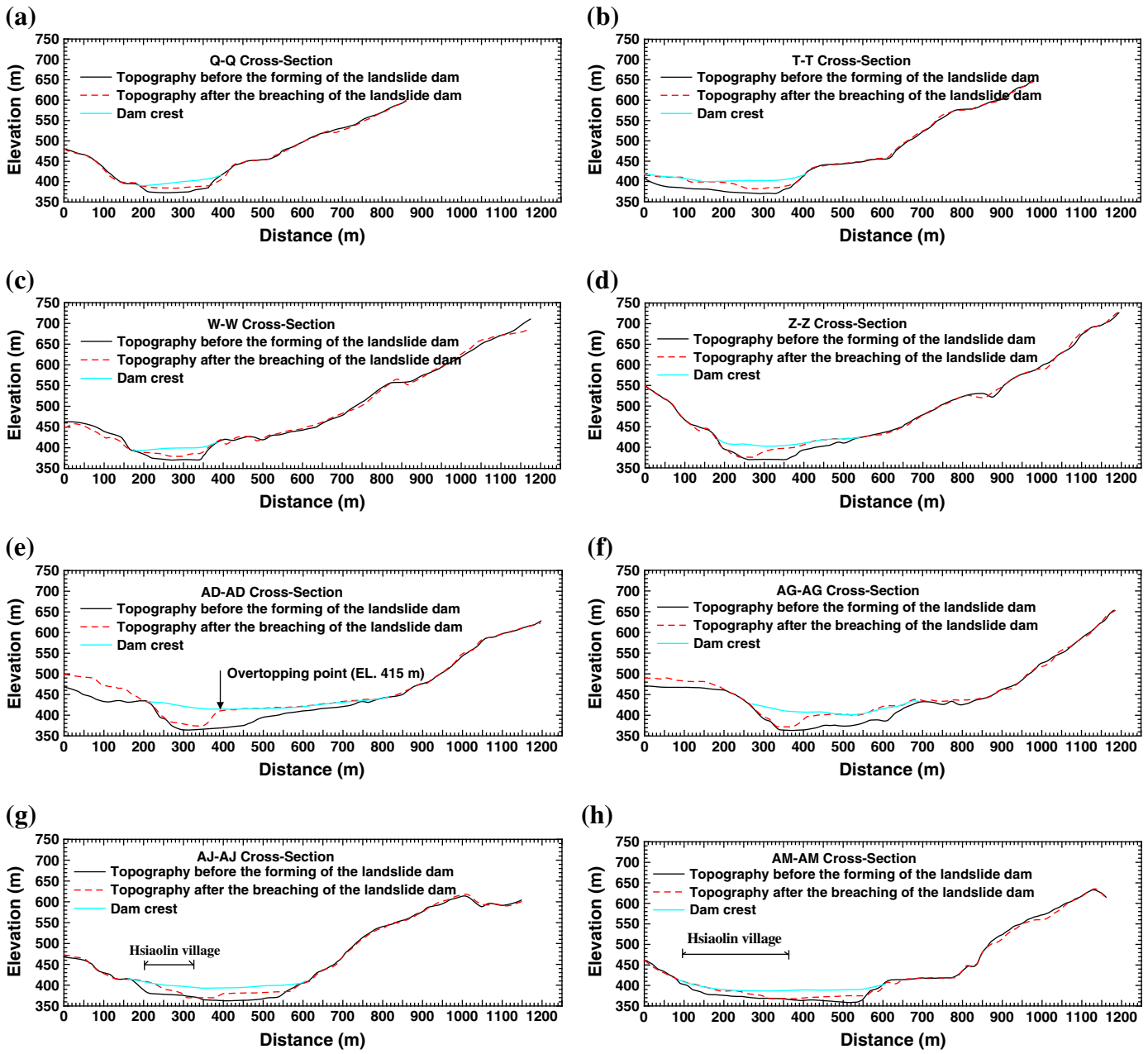


**Fig. 14.** Cross-sections of the Hsiaolin SLD. Solid black lines indicate the topography before the formation of the landslide dam. Dashed red lines show the topography after the dam breach. The blue lines are the inferred dam crest before the dam breach.

(left side of the profiles) can be seen in Fig. 14(e) (AD–AD cross-section) and (f) (AG–AG cross-section). The increased ground-surface elevations of these two cross-sections are due to the large amount of debris that was deposited on creek A (Figure 13). The blue lines in Fig. 14(a)–(h) are the inferred crest of the dam before its breach. Based on the inferred cross-sections, we interpolated the elevation of dam crest and built a DEM representing the topography before the dam breach (Figure 14). As stated previously, the moving mass was split into two slidings, one along creek A and the other along creek B. The largest part of the landslide traveled down along creek A and formed the main body of the landslide dam, which is called "Dam A" in this study. A much smaller dam (called Dam B) was contributed from creek B. The W–W section (Figure 14(c)) is the boundary between Dam A and Dam B. Fig. 14(a)–(b) and (d)–(h) shows the cross-sections of Dam B and Dam A, respectively. A saddle with an elevation of 415 m (marked with a star), where overtopping might have occurred, can be seen at Dam A in Fig. 15. The location of the overtopping point is also indicated in the AD–AD cross-section (Figure 14(e)).

### 6.2. The reconstructed dam shape

The difference between the topography before the landslide (real data) and after the formation of the landslide dam (modeled results) indicates the dam shape (color contours in Figure 15). Fig. 15 shows that the maximum deposition thickness was about 60 m where creek A flowed into Cishan River. We plotted a profile along the dam axis (Figure 16). Two peaks in Fig. 16 represent Dams A and B. The separation point between Dam A and Dam B is at about 450 m in distance from the upstream boundary. The volumes of Dam A and Dam B are 13.2 and $2.2 \times 10^6$ $m^3$, respectively. The total dam volume is

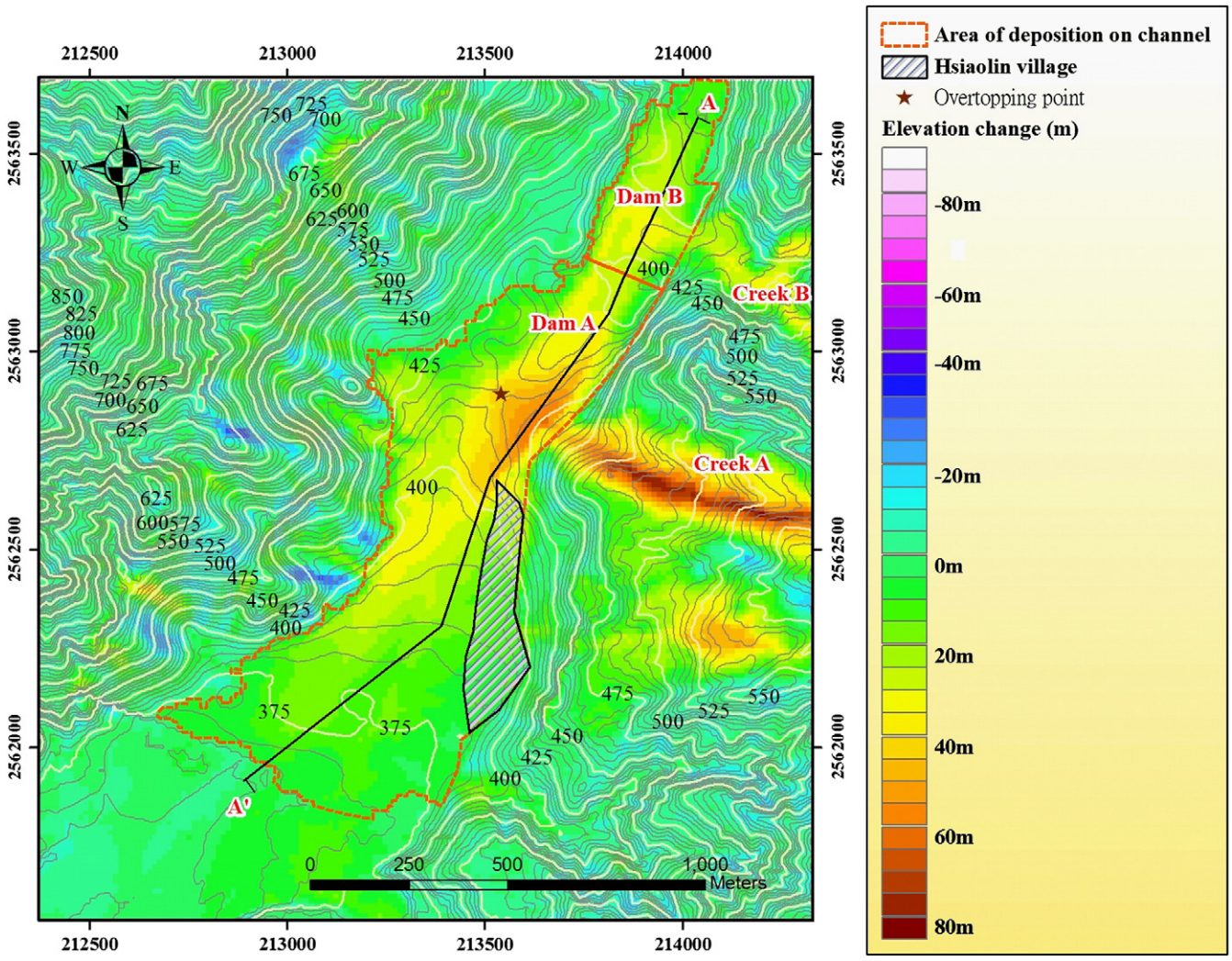


**Fig. 15.** The reconstructed topography (elevation of the dam crest) and inferred deposition thickness of the Hsiaolin SLD (color contours) after the deposition of the landslide and before the dam breach.

$15.4 \times 10^6$ m$^3$, which is very close to the estimated volume of the debris that entered the channel.

### 6.3. Geometry of the landslide dam before and after the breach

The differences in the topography before and after the dam breach indicate the breached dam thickness that is shown in Fig. 17. The breached dam volume is calculated as $7.4 \times 10^6$ m$^3$. That is, about 48% of the landslide dam was washed away. The breached part of the landslide dam is near the east bank of Cishan River, and the breach path is clearly directly toward the Hsiaolin village on the east bank of Cishan River.

## 7. Discussion

### 7.1. Uncertainty related to the reconstruction of the dam geometry

The methodology and data used for reconstructing the geometry of Hsiaolin SLD are summarized in Table 3. Several factors introduced

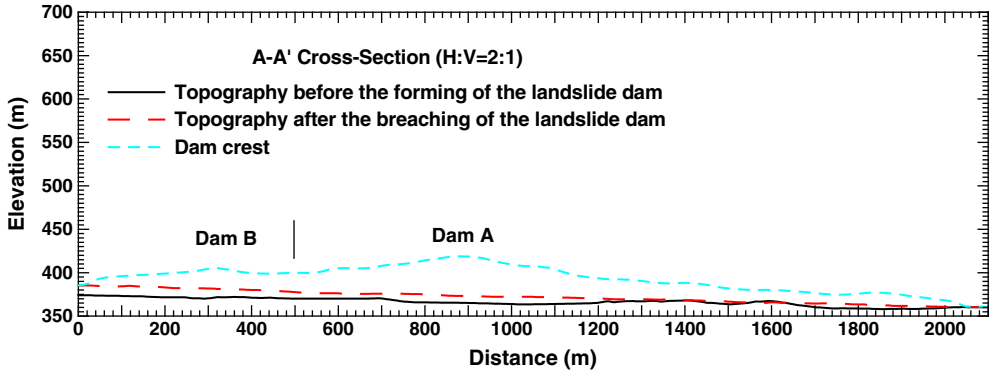


**Fig. 16.** A profile along the river (A-A′). The arrowmarks are the separation point between Dam A and Dam B.

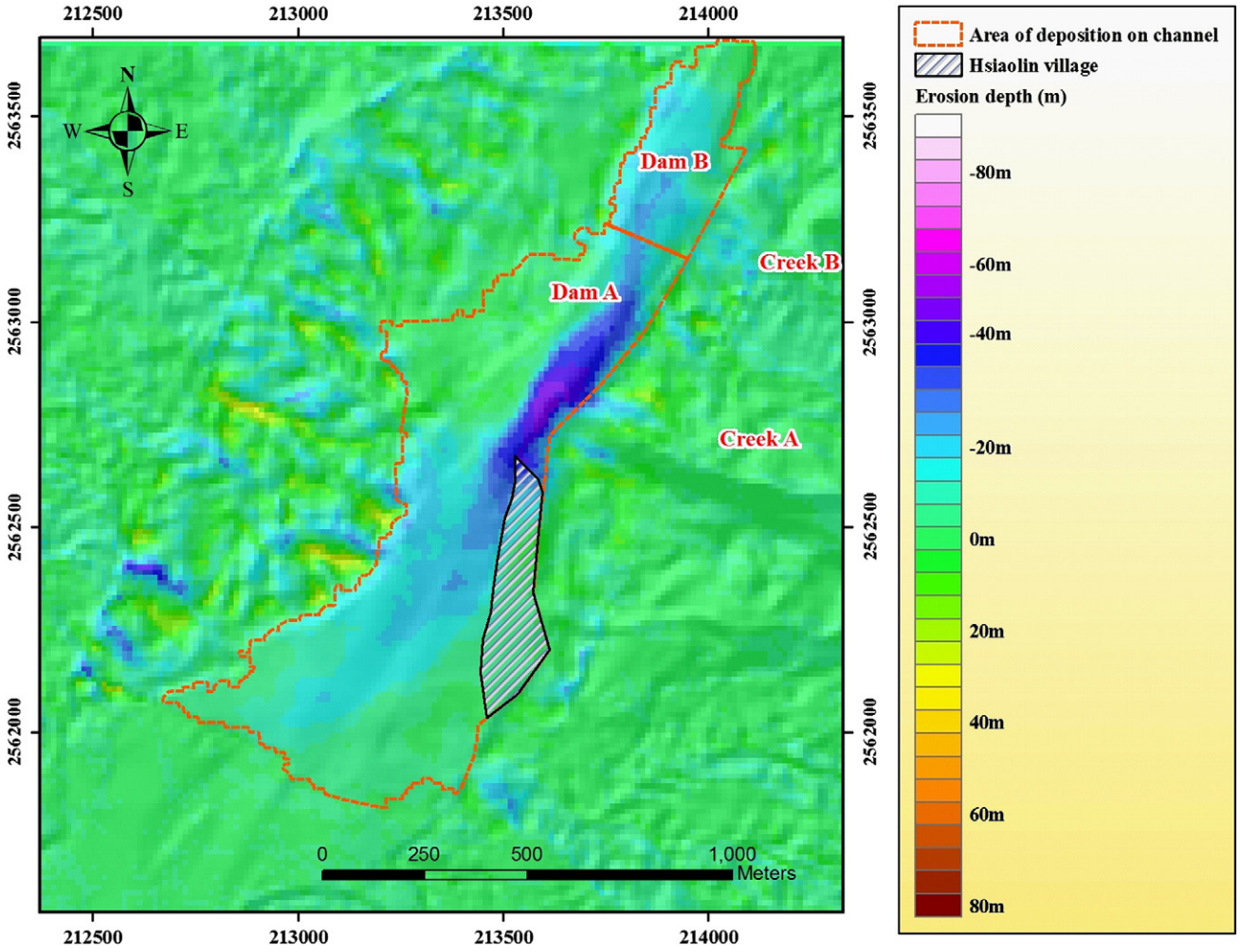


**Fig. 17.** The breached thickness of the Hsiaolin SLD.

uncertainty in the reconstruction of the dam geometry. Those factors (related to the analysis of field evidence, the debris budget and the time to overtopping) are discussed below.

*7.1.1. Field evidence*

The highest elevation of the stripped area on the west bank of the Cishan River was used to reconstruct the dam geometry. Because the action of landslide run-up and the shallow landslides induced by lateral erosion along the riverbank would have stripped the vegetation, the boundary of the landslide dam is difficult to determine. Accordingly, the boundary determined from the bare area is the upper boundary of the extension of the landslide dam.

Field evidence constrains the elevation of dam crest where overtopping occurred to greater than Ele. 410 m (Figure 6) and lower than Ele. 440 m (Figure 7). Eyewitnesses documented that the water reached as far as the No. 11 Bridge, where the elevation is Ele. 425 m to Ele. 430 m. The maximum water level of the landslide lake should thus be less than Ele. 430 m. Based on the run-off simulation and lake storage analysis, the elevation of the dam crests where overtopping occurred is 410–420 m. A rate of three times the simulated flow rate is required to fill the lake to Ele. 440 m about one hour (according to eyewitness reports and broadband seismograms records, overtopping occurred 44–84 min after the dam was formed). It is speculated that the water trace seen at Ele. 440 m might have resulted from a local pounded lake or from surface run-off, possibly from the small gully behind the house in Fig. 7, which could have temporally collected surface run-off blocked by the debris.

A good-quality topographic map is required for geomorphic analysis. In this research, aerial photographs and 5-m-resolution digital terrain models (DEMs) with vertical precision of about 2.5 m were utilized. The influence of vegetation on DEM precision is considered in the standard procedure for producing a DEM by the Aerial Survey Office, Forestry Bureau, Taiwan. However, dense vegetation still affects the geomorphic analysis and induces uncertainty when reconstructing dam geometry. The error induced by the vegetation would likely be reduced if a high-precision Lidar DEM were available.

*7.1.2. Debris budget*

When calculating the debris budget from Eqs. (1) and (2), two factors ($F_F$ and $F_w$) are the most difficult to evaluate. The uncertainty for estimating $F_F$ comes from the unknown volume of the colluvium deposited at the source area. If the sliding mass in the source area were composed only of bedrock materials (without colluvium), the volume expansion due to fragmentation $F_F$ would be 20% and the proportion of materials that entered the channel would be 6% greater than the estimated value ($F_F = 13\%$). However, the estimation of $F_F$ likely induced only minor influence on the reconstruction of dam geometry.

The relative uncertainty for estimating the dam volume that results from the unknown $F_w$ ($0 \le F_w < 1$) is much greater. It is difficult to verify the assumption that all of the debris that entered the blockage channel contributed to the Hsiaolin landslide dam (i.e., $F_w = 0$). However, comparison between the landslide volume and

**Table 3**
Methodology and data used for reconstructing the geometry of the Hsiaolin SLD.

| Reconstructed dam characteristics (related analysis) | Issues related to analysis | Data used or related assumptions |
|---|---|---|
| Dam volume (debris budget) | 1. Topography before landsliding and after dam breaching | 1. 5-m resolution DEMs |
| | 2. Decompaction coefficient of rocks | 2. Case history with similar geological conditions |
| | 3. Volume fraction of rocks and colluvium | 3. Geological model |
| | 4. Fractional amount accounting for the landslide deposits that entered the channel and contributed to the landslide dam | 4. Assuming 100% contribution |
| Dam height at the overtopping point (field evidence + time to overtopping) | 1. Maximum water level of the landslide lake | 1. Field evidence |
| | 2. Flow-rate estimation during the period of damming lake impounding | 2. Rainfall-runoff simulations |
| | 3. Maximum impounding volume of the landslide lake | 3. 5-m resolution DEMs |
| | 4. Time to overtopping | 4. Eyewitness |
| Dam geometry (field evidence + debris budget + time to overtopping) | 1. Boundaries of the deposition height on the river banks | 1. Field evidence |
| | 2. Dam volume | 2. Debris-budget analysis |
| | 3. Dam height | 3. Time-to-overtopping analysis |

dam volume might provide insight as to the reasonableness of this assumption. Ermini and Casagli (2003) documented that, for rainfall-triggered landslides, the mean landslide volume is $31.1\times10^6$ m$^3$ and the mean dam volume is $15.1\times10^6$ m$^3$. This means that the proportion of a landslide that contributes to a blockage is about 50%. For the case of Hsiaolin, the landslide volume is $25.2\times10^6$ m$^3$. Assuming that $F_w=0$ for Hsiaolin landslide dam yields a reasonable, but slightly higher, ratio of ~60%, because the total dam volume (Dams A and B) is $15.4\times10^6$ m$^3$.

The proportion of a dam volume that is contributed from a landslide is determined by the triggering factor (such as earthquakes, rainfall or snowmelt), the landslide type and the landslide volume. Ermini and Casagli (2003) reported that the volume of a rainfall-triggered landslide that contributes to a landslide dam is smaller than that of a seismically triggered landslide. The authors suggested that seismically triggered landslides frequently displace larger volumes of material compared to those induced by rainfall events and that, therefore, the proportion of the landslide that reaches the valley bottom and contributes to the blockage is greater. In this research, we demonstrated that the landslide materials, the rock-mass dilation, the amount of debris entrainment and the deposit that remained on slope all affected the ratio of landslide volume to dam volume. In addition to the aforementioned influence factors, it is suggested that the sliding velocity of moving debris and the flow rate of the river before the blockage should also be taken into account when estimating the debris budget. For the Hsiaolin case, the high moving velocity of the landslide (Tsou et al., 2011) might account for the higher proportion of the landslide that contributed to the blockage.

*7.1.3. Time to overtopping*

In Section 4.3, we calculated the maximum dam volume. Based on the field work, the dam can be considered to have two parts, Dam A and Dam B. Dam A, with a volume of $13.2\times10^6$ m$^3$, was formed from the main part of the landslide. In Section 5, we demonstrated the water storage volume versus the assumed dam height and calculated the corresponding overtopping time. To accurately estimate the overtopping time, the influence of Dam B must also be considered. The volume of Dam B, where it formed at the upstream portion of Dam A, is $2.2\times10^6$ m$^3$. That is, the existence of Dam B would have reduced the storage volume of the main landslide dam, Dam A.

Fig. 18 shows the relationship between the elevation of the impoundment surface and the water storage volume with and without considering the effects of Dam B. It is notable that the water-storage volume of the landslide dam under certain crest heights is overestimated if the effect of dam B is ignored. The overtopping time is also overestimated (Figure 19). For example, if the elevation of the dam crest is 415 m, the estimated overtopping times are 55 min and 69 min, respectively, when considering and neglecting the effect of Dam B. Neglecting the effect of Dam B induced a 25% overestimation in the overtopping time. There is a documented overtopping time of 44 min, and the inferred dam heights are 42 m (at Ele. 413 m) and 36 m (at Ele. 407 m), respectively, with and without the effect of Dam B. That is, a smaller dam height (14% underestimation) will result if the effect of Dam B is neglected.

To determine the dam height from the overtopping time, the water that existed in the channel before the dam formed should also be considered. The elevation of the water-flow surface was not horizontal. For simplicity, if we assume a horizontal water surface with an elevation of 390 m, the pre-existing water volume was $1\times10^6$ m$^3$. This would result in a shorter overtopping time by about 5 min. The influence of the effect of pre-existing water on the dam height estimation would be less than 3 m. The other uncertainty for estimating the elevation of the dam crest from the overtopping time comes from the simulation of the flow rate. However, this issue is beyond the scope of this study.

*7.2. Towards a standardization of the descriptive characteristics of a landslide dam and related lake — the example of the Hsiaolin*

Based on the results of the landslide reconstruction, the detailed information relating to the landslide dam is summarized in Table 4. The methods utilized are also listed. The definitions of the derived variables that are related to the landslide dam can be found in Dong et al. (2009). Key issues relating to these descriptive characteristics of

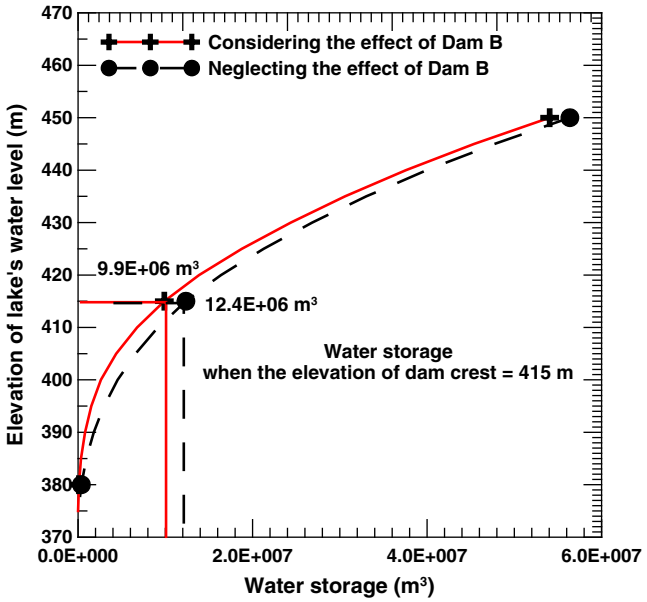


**Fig. 18.** The volume of impounded water versus the different elevations of the dam crest (overtopping point).

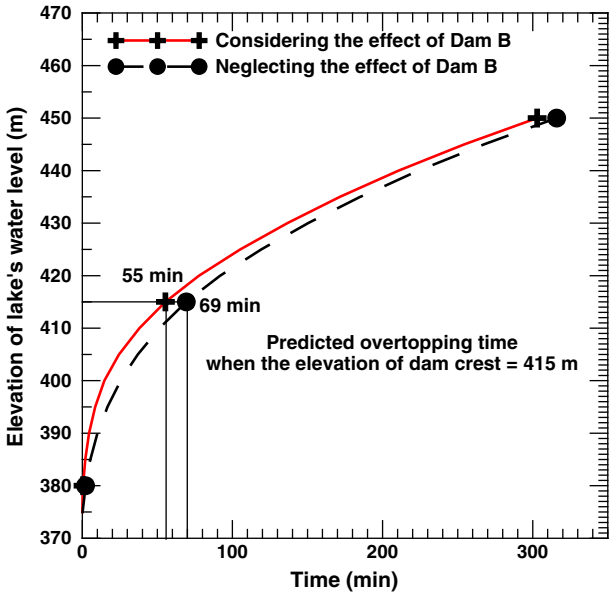


**Fig. 19.** The overtopping time versus the different elevations of the dam crest (overtopping point) under the simulated discharge of 2974 $m^3/s$.

the inferred dam and the resultant lake, as well as the implications for dam stability assessments, are discussed below.

*7.2.1. Issues relating to the descriptive characteristics of a landslide dam*

(1) Frequently, the literature provided inadequate information about dam geometry (for example only a single value or at best a range of values of dam heights). The height of a landslide dam is difficult to determine because the mass normally exhibits a complex geometry. In this research, we suggest that the saddle point on the dam crest (where the overtopping first occurred) could be a reference point to measure the dam geometry. Accordingly, the definitions of dam height and length are clearly specified in this research. In addition, the maximum dam height and length, which are defined as the greatest thickness and the maximum cross-river length of the landslide deposition, are also provided.

(2) Dam volumes documented in landslide dam inventories have sometimes been estimated by $V_d = 0.5 \cdot W_d \cdot L_d \cdot H_d$ (Tabata et al., 2002). According to this simple equation (maximum dam width, length and height), the volume of the Hsiaolin landslide dam would be $22.5 \times 10^6$ $m^3$. The dam volume would be overestimated (with an error of 46%) using this method. That is, adopting an oversimplified geometry of a landslide dam to estimate its volume could induce unacceptable error.

(3) It is difficult to define the lake area, depth and storage volume of a rapidly breached landslide dam. Therefore, we estimated a lake area, depth and impoundment volume according to the Ele. 415 m where the overtopping first occurred.

(4) The simulated peak flow of the Cishan River during Typhoon Morakot is about 5000 $m^3/s$ (Li et al., this issue). However, this peak flow occurred before the formation of the landslide dam. In Table 4, we document a flow rate of 2974 $m^3/s$ as a simulated maximum flow rate for the period relating to the overtopping of the Hsiaolin landslide dam after its formation during Typhoon Morakot.

(5) The longevity of the landslide dam in Table 4 is estimated from the overtopping time. The breaching time is estimated to be 8.4 min after the overtopping according to a companion paper based on a simulated dam breach hydrograph by BREACH; it is not included in the longevity analysis.

*7.2.2. Implications of the reconstructed dam geometry for building a geomorphologic model for stability assessment of landslide dams*

The index-based approach allows for a first-order estimation of landslide-dam stability and for regional comparison of the geomorphic boundary conditions necessary for landslide dam formation and failure (Korup, 2004). For example, Ermini and Casagli (2003) utilized a geomorphic index (DBI) combining dam height ($H_d$); dam volume ($V_d$) and catchment area ($A_c$) to evaluate the stability of a landslide dam, where:

$$\mathrm{DBI} = log\left(\frac{H_d \cdot A_c}{V_d}\right). \quad (3)$$

**Table 4**
Geomorphic variables recorded for the Hsiaolin SLD (definitions of the variables can be found in Dong et al., 2009).

| Variables (reliability level) | Description (method used for deriving the variables) |
|---|---|
| Location (H) | E120°38′39.1″, N23°10′0.6″[a] |
| Catchment area (H) | 354 $km^2$[a] |
| Stream order (H) | 3 (counted from the topographical maps (1/25 000)) |
| Mean flow (H) | 30.13 $m^3/s$ (Mean daily flow at the Nanfeng Bridge stream gage station near the landslide dam site from 1997 to 2008) |
| Peak flow (M) | 2974 $m^3/s$(Inflow rate at the instant when the dam was formed during Typhoon Morakot; from the rainfall-runoff simulation; maximum flow rate of the landslide dam ever sustained) |
| Upstream channel gradient (H) | 7.6%[a] |
| Downstream channel gradient (H) | 1.0%[a] |
| Landslide volume (H) | $25.2 \times 10^6$ $m^3$ (volume of debris entrained and deposited on the slope excluded)[b] |
| Landslide area (H) | 0.62 $km^2$[b] |
| Horizontal travel distance (H) | 2.92 km[c] |
| Slope height (H) | 0.88 km[c] |
| Dam height (M) | 60 m and 44 m (maximum dam height and dam height where the overtopping first occurred)[d] |
| Dam width (M) | 1500 m[d] |
| Dam length (M) | 500 m and 370 m (maximum dam length and the dam length where the overtopping first occurred)[d] |
| Dam volume (M) | 13.2 and $2.2 \times 10^6$ $m^3$ (Dam A and Dam B) (based on the debris-budget analysis) |
| Lake depth (L) | 35 m (maximum water level when overtopping) (inferred from the dam height) |
| Lake area (L) | 0.73 $km^2$ (maximum water level when overtopping) (inferred from the dam height) |
| Lake volume (L) | $9.9 \times 10^6$ $m^3$ (maximum water level when overtopping) (inferred from the dam height) |
| Longevity (M) | 44-84 min (time of the landslide quake registered by the Seismic Network and overtopping time reported by the eyewitnesses, broadband seismograms data and hydrological analysis) |

[a] Derived from a 5-m resolution DEM from before Typhoon Morakot.
[c] Derived from a 5-m resolution DEM from after Typhoon Morakot.
[b] Calculated from 5-m resolution DEMs from before and after Typhoon Morakot.
[d] Calculated from the elevation of the reconstructed dam crest and a 5-m resolution DEM from before Typhoon Morakot.

A dam with a DBI <2.75 will be classified as a stable dam and one with a DBI >3.08 will be classified as an unstable dam. Dong et al. (2009) utilized discriminant analysis to determine that the dominant variables that affect the stability of a landslide dam (in order of relative importance) are peak flow, dam height, width and length. The proposed multivariate regression model is as follows:

$$D_s = -2.94\ log(P) - 4.58\ log(H_d) + 4.17\ log(W_d) + 2.39\ log(L_d) - 2.52 \quad (4)$$

where $D_s$ is the discriminant score (if $D_s$ >0, then the dam is categorized as within the stable group; otherwise, it is placed in the unstable group) and $P$ (in $m^3/s$), $H_d$ (in m), $W_d$ (in m) and $L_d$ (in m) are the peak flow, dam height, width and length, respectively.

For evaluating the dam stability soon after its formation based on those geomorphologic approaches, assessment of the dominating geomorphologic parameters is critical. First of all (as shown in the Hsiaolin case), an estimation of the dam volume could induce error if it is assumed that the dam volume equals the landslide volume or if an oversimplified equation (such as $V_d = 0.5 \cdot W_d \cdot L_d \cdot H_d$) is used. The geological conditions, topography, sliding path, velocity of moving mass and river flow rate affect the contributions of the landslide to the dam volume. Consequently, the dam volume should be calculated from the DEMs before and after the dam formation (if such DEMs are available). When deriving a geomorphologic model for the dam stability assessment, the method used to estimate the dam volume in the landslide dam inventory should be checked carefully.

Second, several definitions were provided in the literature for describing the dimensions of a landslide dam. In this research, we define a dam height and length based on the point where the overtopping first occurred. Because the stability of a landslide dam is closely related to the water level of the impoundment, using dam dimensions related to the dam crest where the overtopping first occurred is suggested to assess the stability of a landslide dam.

Finally, for the Hsiaolin case, the simulated inflow rate for the instance when the dam was formed (2974 $m^3/s$), which was the greatest that the landslide dam ever sustained, is quite different from the maximum flow rate (about 5000 $m^3/s$). When using the peak discharge documented in a landslide-dam inventory to build a statistical model, such as Eq. (4), attention should be paid to minimize the induced error.

Korup (2002) concluded that the lack of standardized descriptive geomorphic characteristics of landslide dams renders quantification of their geomorphic impacts difficult. The aforementioned issues that were learned from the Hsiaolin case could be helpful for further studies that aim to standardize the descriptive geomorphic data related to assessing the risks associated with landslide dams.

#### 7.2.3. Reliability of the inferred geomorphic characteristics of the Hsiaolin landslide dam and the related lake

A complete documentation of the landslide dam case should include the reliability of the geomorphic characteristics. Tabata et al. (2002) studied 79 landslide-dam events that occurred in Japan. The reliability of those landslide dams was categorized into three levels, as follows: (1) high reliability (characteristics of the landslides, dams and lakes are well documented or can be accurately determined from topographical maps); (2) medium reliability (landslides and dams can be accurately located, but the uncertainty surrounding the variables is higher than in category A); and (3) low reliability (the landslides and dams cannot be accurately located, and the reliability of the data is low). In this research, we defined the reliability of each of the variables related to the Hsiaolin SLD. A high reliability (H) indicated that the geomorphic characteristic was determined from topographical data as defined by Tabata et al. (2002). Observed quantities, such as the mean flow, were categorized at the H level. If the quantity was derived from uncertain models, then the derived characteristics were categorized as medium reliability. For example, the dam height, width and length were inferred from dam volume and time to overtopping. Accordingly, those variables have a medium reliability. If a variable was derived from an inferred variable of the level M, then the reliability was categorized as low. For example, the lake-related characteristics were inferred from dam height, and we categorized their reliability level as L. The reliabilities of the inferred geomorphic characteristics are indicated in Table 4.

### 7.3. Possible failure mechanisms for the breached Hsiaolin landslide dam

Three failure mechanisms are considered to determine the instability of landslide dams: overtopping, piping and slope failure (Schuster and Costa, 1986; Swanson et al., 1986). Of these, overtopping is the most important (Schuster and Costa, 1986). It is logical to postulate that the failure mechanism of the Hsiaolin landslide dam was due to overtopping because eyewitnesses documented that the dam collapsed soon after the overtopping. Two additional factors also indicate that overtopping might have dominated the failure of the Hsiaolin landslide. (1) The dam materials were mainly composed of impermeable fine particles, and the lifetime of the Hsiaolin landslide dam was only about an hour. For piping, one hour is too short, and thus the possibility that the dam failure is related to piping is low. (2) The downstream slope of the landslide dam was less than 10% (about 5°). This gentle slope is rather stable even when considering that seepage likely induced pore pressure.

To evaluate quantitatively the possible failure mechanism of the Hsiaolin landslide dam, a 2D model for seepage analysis and slope stability analysis was built based on the dam geometry reconstruction. SLIDE 5.0 (developed by Rocscience Inc.) was utilized to calculate the hydraulic gradient at the toe of the downstream surface of the landslide dam. In addition, the slope stability of the landslide dam was calculated considering the influence of pore water pressure from the seepage analysis. The top boundary of the model (dam surface) was determined from the inferred dam geometry. The elevation of the bedrock in the river channel was assumed as the bottom boundary. In addition to the dam materials (material 1), a layer composed of alluvium (material 2) covered the bedrock and underlay the landslide dam. Based on the post-investigation at the breached dam site, Chen, 2011 reported that the thickness of the alluvium was about 15 m. Accordingly, the bottom of the numerical model (bedrocks) was set at an elevation 15 m lower than that of the surface elevation that was read from the DEM before Typhoon Morakot. For seepage analysis, the left (south) side and bottom of the model were assumed to be impermeable. A constant total head (415 m) was assumed for the right (north) boundary and for the upstream side of the dam surface. The downstream side of the dam surface was assumed to be a seepage face where the pressure head equaled 0. The model geometry and the boundary conditions are shown in Fig. 20 (central part). The material properties that were used for the seepage analysis and the slope stability analysis are listed in Table 5. Notably, the strength parameters of material 1 are selected from a dataset reporting the strength of colluvium and gravelly soils (WRPI, 2003) with lowest value.

The pore pressure and vertical hydraulic gradient distributed in the landslide dam were determined according to the seepage analysis. The lower portion of Fig. 20 indicates that the vertical hydraulic gradient (color contours) at the toe of the Hsiaolin landslide dam was below 0.1. This is much lower than the critical hydraulic gradient (1.0) for the occurrence of piping. Considering the pore pressure that was distributed in the landslide dam (color contours in the upper portion of Figure 20), the calculated safety factor was about 3.2. This indicates that the failure of the Hsiaolin landslide dam was not induced by the slope instability.

It is notable that the upper part of the dam was mainly composed of permeable large blocks that were not considered in the seepage

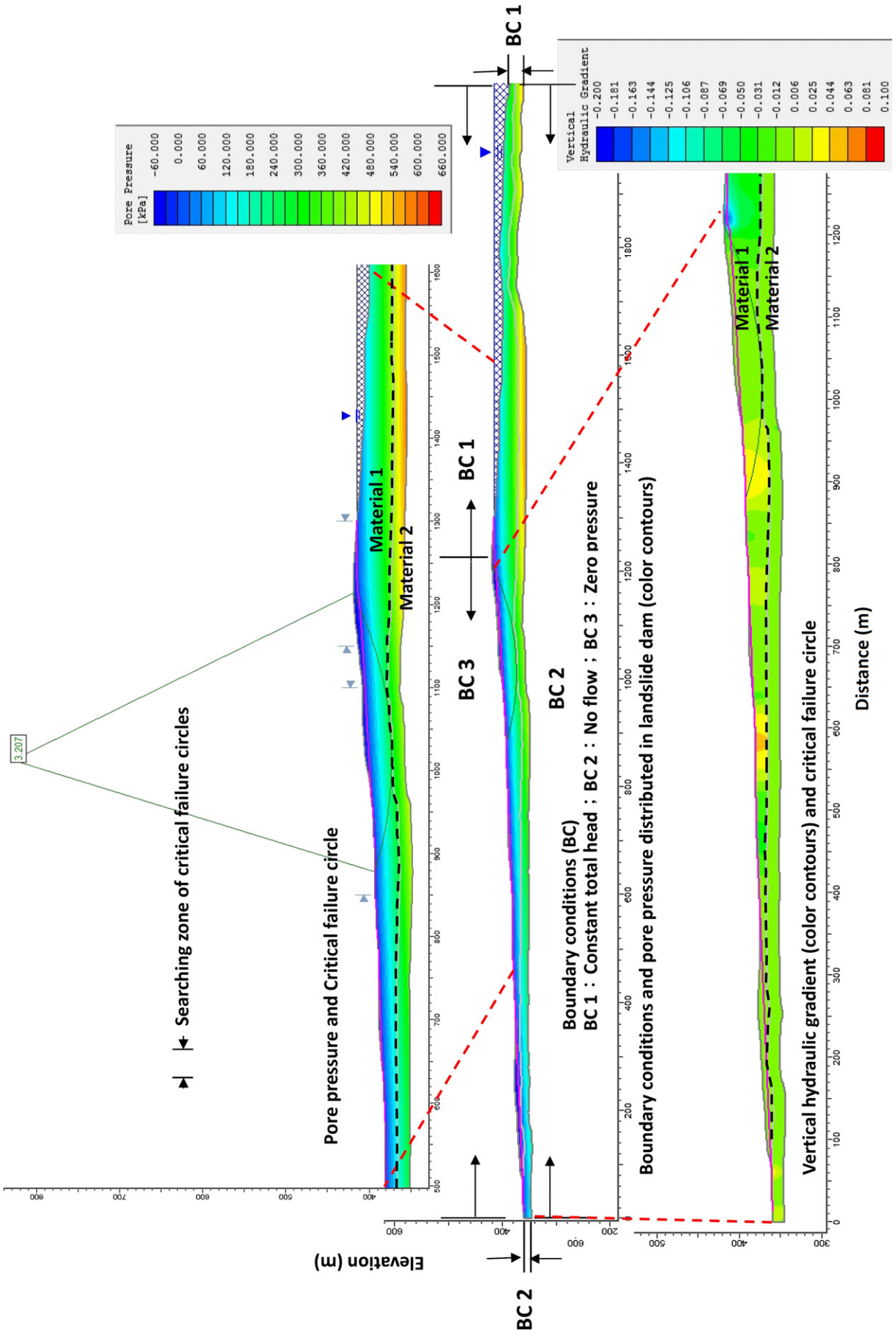


**Fig. 20.** The seepage analysis and slope stability analysis of the Hsiaolin landslide dam.

**Table 5**
Input parameters for seepage analysis and slope stability analysis of the Hsiaolin landslide dam.

| | Material 1 (Dam) | Material 2 (alluvium) |
|---|---|---|
| Unit weight (kN/m$^3$) | 20.6 [a] | 20.9 [b] |
| Cohesion (kPa) | 6 [c] | 0 [b] |
| Friction angle (degree) | 22 [c] | 37 [b] |
| Hydraulic conductivity (cm/s) | $10^{-5}$ [d] | $10^{-4}$ [e] |

[a] Averaged unit weight of samples from Hsiaolin landslide dam.
[b] Averaged parameters of gravelly soils (WRPI, 2003).
[c] Lowest strength parameters of colluvium (WRPI, 2003).
[d] Silty–clayey sands (Fetter, 1994).
[e] Assumed value.

analysis. One possible dam-failure scenario is postulated as follows. The water level first reached the permeable layer and the observable seepage flow began to erode the underlying fine material. High-velocity seepage at the top permeable layer might have accelerated the breaching process. This scenario accounts for why the overtopping time documented by the eyewitness was so short.

## 8. Conclusions

Aerial photographs, high precision DEMs, as well as laboratory work and extensive field-investigation results were used to reconstruct the short-lived Hsiaolin landslide dam with successful results. The overtopping time of the landslide dam and the balance of the debris budget were also used to determine the dam geometry. Based on the multi-disciplinary technologies used, the total volume of the Hsiaolin landslide is estimated to be $25.2\times10^6$ m$^3$. The total volume of the landslide dam was estimated to be $15.4\times10^6$ m$^3$. Only half of the sliding mass contributed to the main body of the landslide dam even when the rock-mass dilation and debris entrainment were considered. The maximum elevation attained by the run-up landslide deposition was Ele. 475 m (on the west bank of the Cishan River), but the elevation of the maximum water level or the dam crest where overtopping occurred was Ele. 415 m (at the center of the river course). Using this definition, the dam height was 44 m, and the deepest deposit was 60 m thick. The cross-river length passing through the overtopping point is 370 m. The maximum cross-river length (crest length) and the along-river width of the dam were 500 m and 1500 m, respectively. Regarding the hydrological characteristics related to the landslide dam and the impounded lake, the catchment area on the upstream of the landslide dam was 354 km$^2$ and the maximum volume of impounded water before the overtopping occurred was $9.9\times10^6$ m$^3$. Based on the 2D rainfall-runoff simulation over the Cishan River basin, the inflow of the Cishan River was 2974 m$^3$/s at the instant when the landslide dam formed.

Uncertainty related to the reconstruction of dam geometry was induced by the analysis of field evidence, the debris budget and the time to overtopping. It is shown that the proportion of the dam volume that was contributed by the landslide is difficult to determine. In addition, neglecting the existence of the smaller Dam B could cause significant error when either inferring the dam geometry or evaluating the time of overtopping. Therefore, reliability of the characteristics related to the landslide, dam and lake should be documented. Three categories of reliability level are proposed. The reliability is categorized as high level if the geomorphic characteristic is determined from topographical data or from an observed quantity. The peak flow and dam geometry with medium reliability are inferred from certain models with assumptions. Because the lake area, depth and volume were indirectly determined from the dam height, the lake-related characteristics are ranked as low reliability.

In this research, a standardized description of landslide-dam characteristics and implications for risk assessment is elucidated. Among other issues, the estimation of the dam volume either from the landslide volume or based on an oversimplified equation could induce unacceptable error. Using the height and length of the landslide dam based on the dam crest where the overtopping first occurred is suggested to assess the stability of a landslide dam. In addition, the peak discharge after the river blockage should be used to assess the dam stability. Based on numerical analysis, the low hydraulic gradient at the toe of the dam's surface and the high safety factor of the dam slope indicate that the piping and slope instability were irrelevant to the failure of the Hsiaolin landslide dam. It is postulated that the overtopping event dominated the failure process. Based on the reconstructed landslide dam geometry, the dam-breach hydrograph and the mudflow could be simulated. The breaching process of the landslide dam is documented in a companion paper of this special issue.

## Acknowledgments

This study was supported by the National Science Council of Taiwan through the National Central University under Grants NSC 98-2745-M-008-013 and NSC 99-2625-M-009-004-MY3. Valuable hydrometeorological data were provided by the Central Weather Bureau and Water Resources Agency in Taiwan. The Aerial photograph and DEMs were provided by the Aerial Survey Office, Forestry Bureau, Taiwan. The authors are grateful for their support. The authors would also like to extend our thanks to Prof. Hsein Juang and two anonymous reviewers for constructive comments that greatly improved the manuscript.

## References

Casagli, N., Ermini, L., 1999. Geomorphic analysis of landslide dams in the Northern Apennine. Transactions of the Japanese Geomorphological Union 20 (3), 219–249.
Casagli, N., Ermini, L., Rosati, G., 2003. Determining grain size distribution of material composing landslide dams in the Northern Apennine: sampling and processing methods. Engineering Geology 69, 83–97.
Chang, K.J., Taboada, A., Chan, Y.C., Dominguez, S., 2006. Post-seismic surface processes in the Jiufengershan landslide area, 1999 Chi–Chi earthquake epicentral zone, Taiwan. Engineering Geology 86, 102–117.
Chen, C.C., Personal communications, 2011.
Chen, S.C., Hsu, C.L., 2009. Landslide dams induced by Typhoon Morakot and its risk assessment. Sino–Geotechnics 122, 77–86 (in Chinese with English abstract).
Chen, R.F., Chang, K.J., Angelier, J., Chan, Y.C., Deffontaines, B., Lee, C.T., Lin, M.L., 2006. Topographical changes revealed by high-resolution airborne LiDAR data: the 1999 Tsaoling landslide induced by the Chi–Chi earthquake. Engineering Geology 88, 160–172.
Costa, J.E., Schuster, R.L., 1988. The formation and failure of natural dam. Geological Society of America Bulletin 100, 1054–1068.
Dong, J.J., Tung, Y.H., Chen, C.C., Liao, J.J., Pan, Y.W., 2009. Discriminant analysis of the geomorphic characteristics and stability of landslide dams. Geomorphology 110, 162–171.
Dong, J.J., Tung, Y.H., Chen, C.C., Liao, J.J., Pan, Y.W., 2011. Logistic regression model for predicting the failure probability of a landslide dam. Engineering Geology 117, 52–61.
Ermini, L., Casagli, N., 2003. Prediction of the behaviour of landslide dams using a geomorphological dimensionless index. Earth Surface Processes and Landforms 28, 31–47.
Fetter, C.W., 1994. Applied hydrogeology, 3rd ed. Prentice Hall, Inc., Upper Saddle River, NJ.
Hazen, A., 1930. Water supply. American Civil Engineers Handbook. John Wiley & Sons, New York, pp. 1444–1518.
Hungr, O., Evans, S.G., 2004. Entrainment of debris in rock avalanches: an analysis of a long run-out mechanism. Geological Society of America Bulletin 116, 1240–1252.
Korup, O., 2002. Recent research on landslide dams — a literature review with special attention to New Zealand. Progress in Physical Geography 26, 206–235.
Korup, O., 2004. Geomorphometric characteristics of New Zealand landslide dams. Engineering Geology 73, 13–35.
Lee, C.T., Dong, J.J., Lin, M.L., 2009. Geological investigation on the catastrophic landslide in Shiaolin Village, Southern Taiwan. Sino–Geotechnics 122, 87–94 (in Chinese with English abstract).
Li, M.H., Sung, R.T., Dong, J.J., Lee, C.T., Chen C.C., submitted for publication-this issue. The formation and breaching of a short-lived landslide dam at Hsiaolin village, Taiwan — Part II: simulation of debris flow with landslide dam breach. Engineering Geology.
Schuster, R.L., Costa, J.E., 1986. A perspective on landslide dams. In: Schuster, R.L. (Ed.), Landslide Dam: Processes Risk and Mitigation. Geotechnical Special Publication, 3. American Society of Civil Engineers, pp. 1–20.

Swanson, F.J., Oyagi, N., Tominaga, M., 1986. Landslide dam in Japan. In: Schuster, R.L. (Ed.), Landslide Dam: Processes Risk and Mitigation. Geotechnical Special Publication, 3. American Society of Civil Engineers, pp. 131–145.
Tabata, S., Mizuyama, T., Inoue, K., 2002. Natural Landslide Dams Hazards. Kokonshoin, Tokyo. (in Japanese).
Tsou, C.Y., Feng, Z.Y., Chigira, M., 2011. Catastrophic landslide induced by Typhoon Morakot, Shiaolin, Taiwan. Geomorphology 127, 166–178.
WRPI, 2003. Study on the disaster mitigation strategies for landslide dams (2/3). Report of Water Resources Planning Institute, Water Resources Agency, MOEA, Taiwan.